2015

High Frequency Resolution Adaptive Thresholding Wideband Receiver System

Feiran Liu
Wright State University

High Frequency Resolution Adaptive Thresholding Wideband Receiver System

A thesis submitted in partial fulfillment

of the requirements for the degree of

Master of Science in Engineering

By

Feiran Liu

B.S., *Dalian Jiaotong University, China*, 2012

2015

WRIGHT STATE UNIVERSITY

WRIGHT STATE UNIVERSITY
GRADUATE SCHOOL

December 15, 2015

I HEREBY RECOMMEND THAT THE THESIS PREPARED UNDER MY SUPERVISION BY Feiran Liu ENTITLED "High Frequency Resolution Adaptive Thresholding Wideband Receiver System" BE ACCEPTED IN PARTIAL FULFILLMENT OF THE REQUIREMENTS FOR THE DEGREE OF Master of Science in Engineering

_____

Henry Chen, Ph.D.
Thesis Director

_____

Brian D. Rigling, Ph.D.
Chair, Department of
Electrical Engineering

Committee on Final Examination

_____

Henry Chen, Ph.D.

_____

Yan Zhuang, Ph.D.

_____

Jiafeng Xie, Ph.D.

_____

Robert E. W. Fyffe, Ph.D.
Vice President for Research and
Dean of the Graduate School

Abstract

Liu, Feiran. M.S.Egr, Department of Electrical Engineering, Wright State University, 2015. “High Frequency Resolution Adaptive Thresholding Wideband Receiver system”.

Fast Fourier transformation (FFT) is widely used in wideband digital receivers to detect multiple signals. To achieve high dynamic range, the receiver has to increase analog-to-digital (ADC) resolution bits, which requires significant computation time and therefore increases receiver time resolution. The other challenge of FFT approach is two signals with a small frequency difference (i.e., less than five FFT frequency bins in most cases) cannot be detected simultaneous. This thesis presents an adaptive thresholding wideband digital receiver to accurately detect two simultaneous high dynamic range signals even when they are close to one FFT frequency bin. The receiver can perform well for more than two input signals if the requirements for the receiver frequency resolution and dynamic range are reduced. The receiver design architecture and performance evaluation are presented.

Table of Contents

List of Figures

List of Tables

Acknowledgement

I would like to thank my advisor, Dr. Henry Chen for his great help on this thesis.

I would also like to express my gratitude to my dear parents. Thank them for raising me, helping me and loving me.

Finally, many thanks to the committee members for giving me the chance to defense this research.

I. Introduction

With the advanced development and pervasive application of communication products, wideband receivers play a much more important role in signal detection and tracking ever than before.

The basic application of a modern wideband receiver is to detect the RF signals with the purpose of distinguishing and analyzing their sources [1]. Generally, signals are different in power and full of noise due to the different searching requirements and complex working environment. Present receivers are not only challenged by quickly intercepting through a very wide frequency band in real time with acceptable sensitivity [2], but also needed to detect multiple signals with a high frequency resolution and instantaneous dynamic range (IDR). Meanwhile, because there is no prior knowledge on the number of signals, the received signals could be ignored incautious, or the result from the receiver could even be false alarm after the normal receiver processing. In this case, new design architecture is presented to accurately detect incoming signals and also the frequency resolution. This thesis is focused on developing general signal detection algorithm and design components that are implemented and verified in Matlab simulation. The hardware implementation will be further studied and verified in the future.

1.1 Fast Fourier Transform

The discrete Fourier transform (DFT) is well known in the past decades because of its extensive use in wireless communication and digital signal processing. This mathematic algorithm could convert the original time-domain signal x (n) with a

length of total input data N to easily analyzed frequency-domain data X (k) by using the following Eq. (1. 1) directly

$$\text{X (k)} = \sum_{n=0}^{N-1} x\,(n)\, e^{-j\,2\pi kn/N},\ 0 \le k \le N-1 \qquad (1.\ 1)$$

Noticing that the N bit DFT requires almost N square times operation. Thus, implementation of DFT always produces intricate and abundant hardware usage.

In the modern receiver design, a much more efficient, faster and easier for hardware implementation way to process digital signal, called fast Fourier transform (FFT), is increasingly taken the place of DFT which has fallible and complex computation procedure. There are amount of different FFT algorithms which can reduce the total operations, such as radix 2, higher radix [3], split radix [4] and mixed radix fast Fourier Transform [5]. The basic fast Fourier transform computational logic separates the N length data to two N/2 length data in every step. In the end of the computation, the same result with the DFT could be got in N*log (2*N) operations from FFT, which could be less than 1 percent of the number of operations of DFT.

To analyze the unknown-frequency input signal x (n) by FFT, the Eq. (1. 1. 1) must be expressed as

$$\text{X (k)} = \sum_{n=0}^{N-1} x\,(n)\, W_N^{kn},\ \ 0 \le k \le N-1 \qquad (1.1.2)$$

$$W_N^{kn} = e^{-j\,2\pi nk/N} \qquad (1.1.3)$$

The W_N^{kn} in the (1.1.2) and (1.1.3) is called the twiddle factor which is the key difficulty to compute the X (k) in DFT algorithm. In order to improve the efficiency of the calculation for this twiddle factor, Euler's formula, expressed in Eq. (1.1.4), is used to rebuild the Eq. (1.2).

$$e^{j\,\theta} = \cos(\theta) + j\sin(\theta) \qquad (1.1.4)$$

After substituting the Euler's formula to the Eq. (1.3), the new twiddle factor equation is

$$W_N^{nk} = \cos\left(\frac{2\pi nk}{N}\right) + j\sin(\frac{2\pi nk}{N}) \tag{1.1.5}$$

From the Eq. (1.1.3), Eq. (1.1.4) and Eq. (1.15), the twiddle factor could be further analyzed to reduce the complexity of calculation.

$$W_N^{n(k+\frac{N}{2})} = e^{-j\,2\pi n(k+\frac{N}{2})/N} \tag{1.1.6}$$

$$W_N^{n(k+\frac{N}{2})} = e^{-j\,2\pi nk}e^{-j\,\pi n} \tag{1.1.7}$$

$$e^{-j\,\pi n} = \cos(-\pi n) + j\,sin(-\pi n) = -1 \tag{1.1.8}$$

Substituting the Eq. (1.1.8) into Eq. (1.1.7), the following formula could be easily achieved.

$$W_N^{n(k+\frac{N}{2})} = -e^{-j\,2\pi nk/N} \tag{1.1.9}$$

$$W_N^{n(k+\frac{N}{2})} = -W_N^{nk} \tag{1.1.10}$$

Thus, the symmetric property of the twiddle factor is exhibited in Eq. (1.1.11).

$$W_N^{k+\frac{N}{2}} = -W_N^{k} \tag{1.1.11}$$

The periodic property of the twiddle factor also could be investigated by making k+N replace k in Eq. (1.1.3). Then the new equation is written as

$$W_N^{n(k+N)} = e^{-j\,2\pi n(k+N)/N} \tag{1.1.12}$$

$$W_N^{n(k+N)} = e^{-j\,2\pi nk/N}e^{-j\,2\pi n} \tag{1.1.13}$$

Similar to the symmetry of twiddle factor, the Eq. (1.1.4) could be written as the formula below.

$$e^{-j\,2\pi n} = \cos(-2\pi n) + j\,sin(-2\pi n) = 1 \tag{1.1.14}$$

By substituting the Eq. (1.1.14) to Eq. (1.1.13), the periodic property of the twiddle factor is shown in the Eq. (1.1.15).

$$W_N^{k+N} = W_N^k \tag{1.1.15}$$

There are two basic types of the FFT computation, the Decimation in Time (DIT) computation method and the Decimation in Frequency (DIF) computation method. The difference between DIT method and DIF method is the position of twiddle factor in the FFT procedure. The twiddle factor of DIT would be used at first, which is shown in Fig 1.1.1. As a comparison, the twiddle factor of DIF is computed at the end of the procedure, which is shown if Fig 1.1.2.

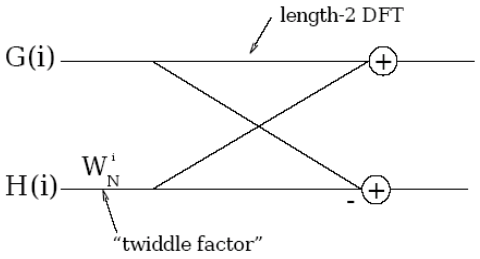

Fig 1.1.1 Decimation in Time (DIT) method

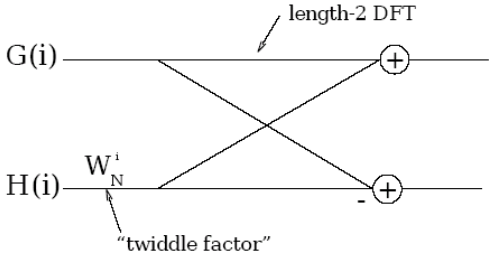

Fig 1.1.1 Decimation in Frequency (DIF) method

Decimation in Time splits the input data x (n) to the odd terms and even terms, which could be expressed as x (0), x (2), x (4)…x (N-2) and x (1), x (3), x (5)…x (N-1). Then the Eq. (1.1.2) could be written as

$$\mathrm{X(k)} = \sum_{n=0}^{\frac{N}{2}-1} x(2n) W_N^{2nk} + \sum_{n=0}^{\frac{N}{2}-1} x(2n+1) W_N^{(2n+1)k} \tag{1.1.16}$$

Noticing the X (k) split in two N/2 point DFT in Eq. (1.1.16) which is called radix-2 FFT algorithm reduce the number of computation stages. Making use of symmetry and periodicity of twiddle factor with further separating the Eq. (1.1.16) to additional odd terms and even terms could decrease the total number of stages from N^2 to (N/2)*$\log_2$(N).

The larger bit of the DFT has, the more computation stages are saved by the FFT algorithm. Fig 1.1.3 and Fig 1.1.4 show the figures of 16 bit DIT and DIF FFT algorithm.

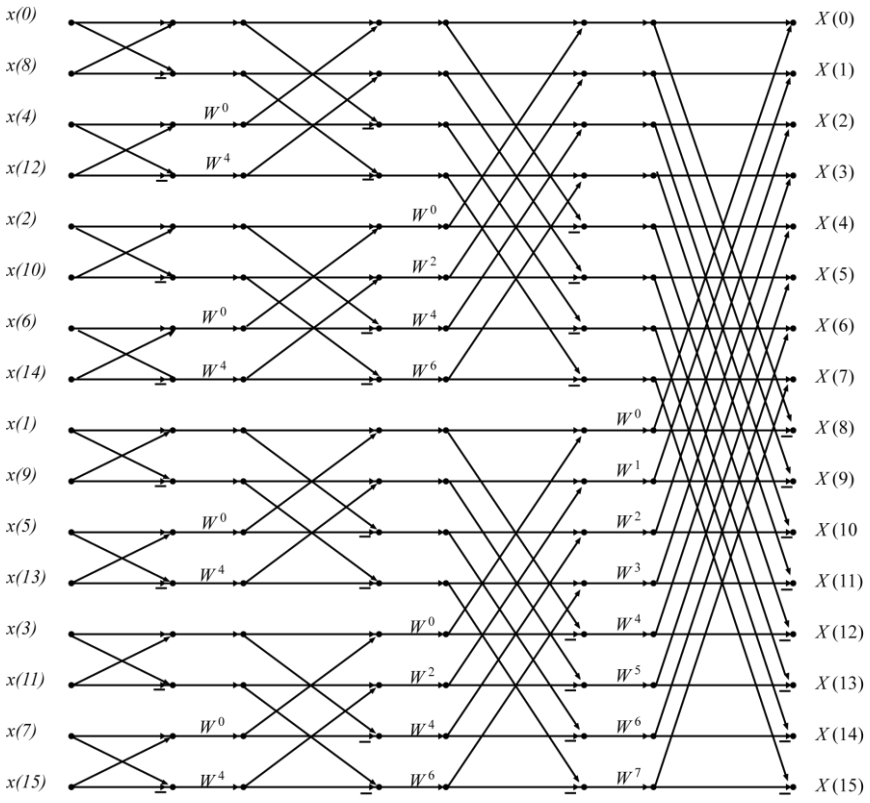

Fig 1.1.2 Decimation in Time (DIT) method for 16 points FFT

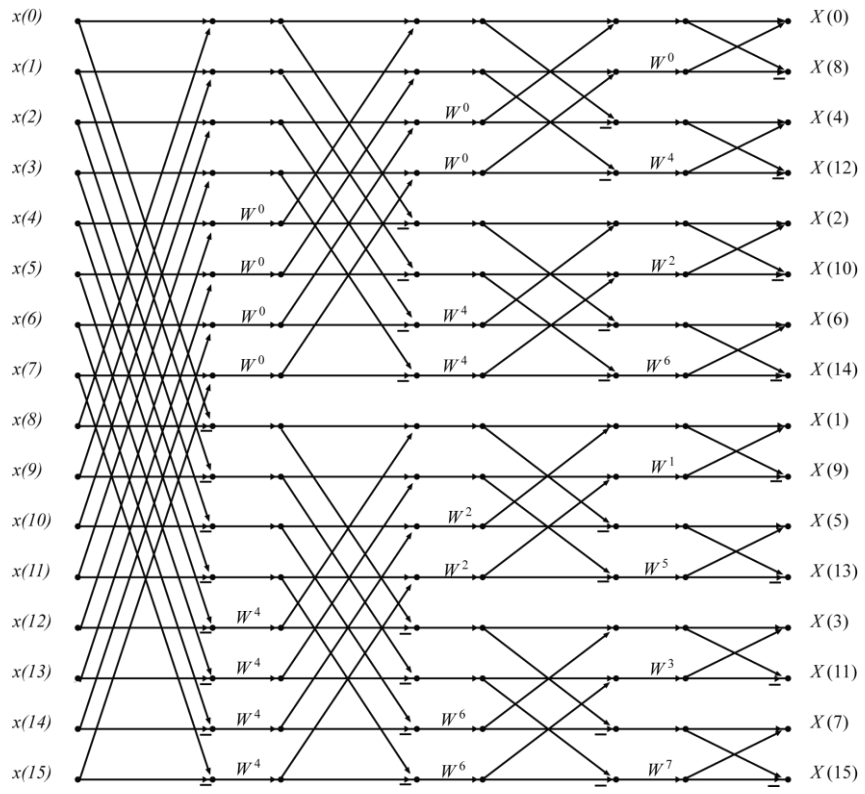

Fig 1.1.3 Decimation in Frequency (DIF) method for 16 points FFT

FFT has a satisfying performance in rapidly analyzing and can determine frequencies of multiple signals so it is introduced in lots of digital receiver architecture designs, such as monobit receiver [6]. This research use the DIT algorithm which is implemented by Matlab.

1.2 Hanning Window Function

There are several well know restrictions for accuracy of FFT based receivers, such as jitter, large frequency which is out of the Nyquist zone and FFT resolution. Another property that always generates errors is the leakage due to the non-periodic data. Ideally, FFT computation algorithm considers the input signal is perfect periodic, which means, the input signal has a small and easy-identified main-lobe. Thus, the frequency of the input data could be located accurately.

Nevertheless, the sampled time domain data is disturbed by the noise or any other signals in the real world, then the FFT spectrum could be distorted and the result could be inaccurate. This phenomenon is called leakage of the FFT. When leakage happens, the energy of the input signal diffuses to a wider frequency range instead of the original narrow frequency range in the FFT spectrum, that is, the main-lobe of the signal is expanded. Fig 1.2.1 shows the comparison of the non-leakage spectrum and the spectrum with leakage.

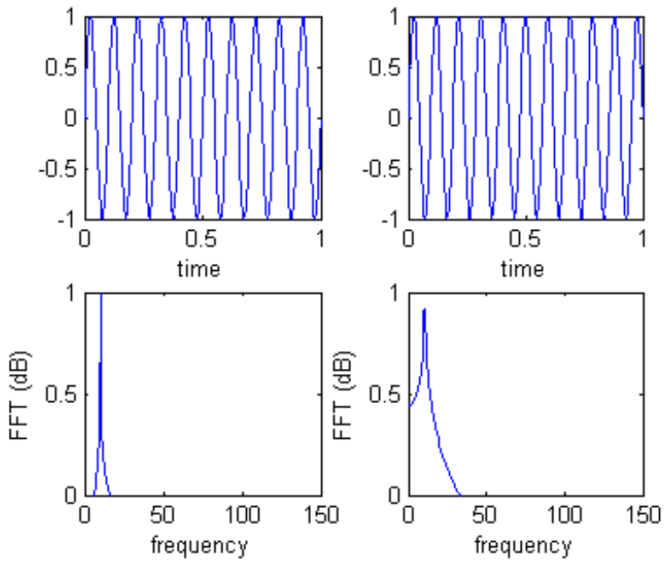

Fig 1.2.1 Comparison of the Non-leakage Spectrum and the Spectrum with Leakage

The left two pictures of Fig 1.2.1 show the property of perfect periodic input signal, and the main-lobe is quite small and no leakage. On the other hand, the main-lobe of the signal power density expands and becomes more dispersed in the right two graphs, which is the effect of leakage.

In order to overcome the effect of leakage and get better result from FFT measurement, a window function must be applied to rectify the errors. The shape of a window is zero at the beginning and end of the whole power spectrum, and exist

particular shape in the middle. Fig 1.2.2 shows four frequently-used window functions.

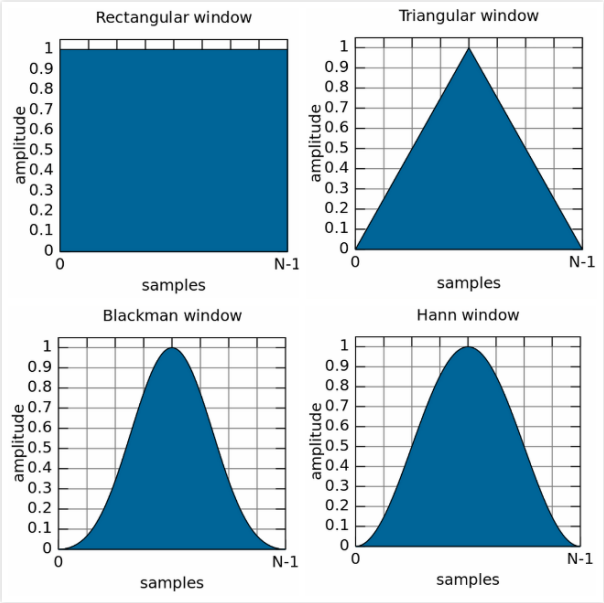

Fig 1.2.2 Frequently-used Window Functions

Hanning window function, also called Hann function, is a reliable chose to reduce the leakage and reshape the signal power spectrum which has low aliasing. Fig 1.2.3 shows the frequency response of the hanning window in FFT.

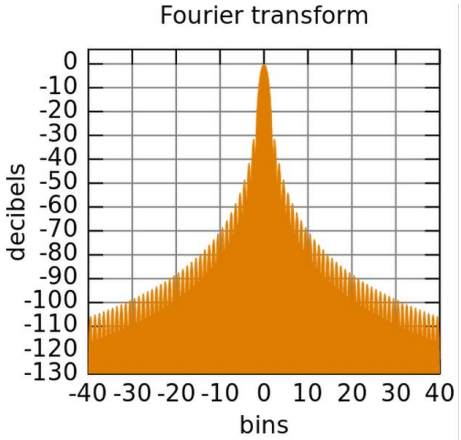

Fig 1.2. 3 Hanning window frequency response in FFT

Although the FFT window functions could not erase leakage exhaustively, the reshaped leakage effectively helps people locate precise frequency. Fig 1.2.4 shows the difference between a non-periodic sine wave to windowed sine wave.

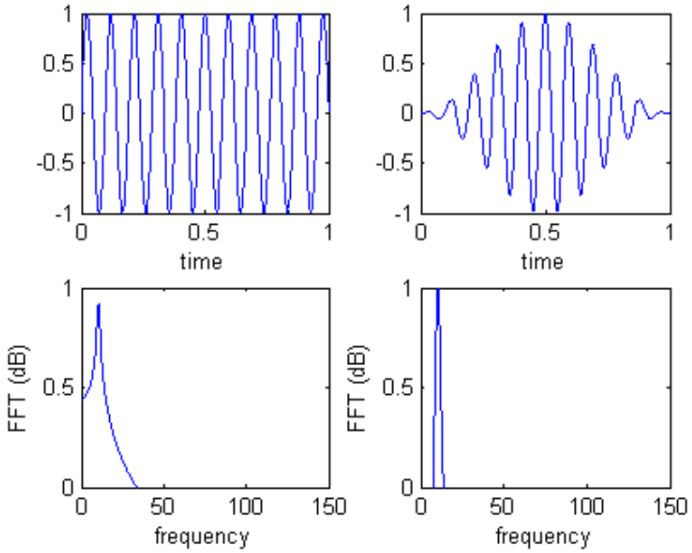

Fig 1.2.4 Non-periodic Sine Wave with Leakage (left) and Reshaped Wave (right)

In this thesis, the scale factor of 1024 is considered as the Hanning window function coefficients. The Hanning window is applied to the time domain data from the ADC by Matlab program, then the windowed data would be analyzed by FFT algorithm.

1.3 Super-resolution Compensation

With the advance of modern communication and sensing technology, detecting multiple signals simultaneously with good instantaneous dynamic range (IDR), high resolution and unexpected number of input signals becomes a non-ignorable requirement for wideband receiver design [7]. As discussed in section 1.2, the Hanning window function could suppressed the side-lobes, which indicates that the

receivable frequency resolution of the receiver is mainly determined by the main-lobe of the windowed signal, especially the wide main-lobe of the strongest signal when several inputs exist [8]. Fig 1.3.1 shows the frequency response in 1024-point FFT spectrum with two input signals.

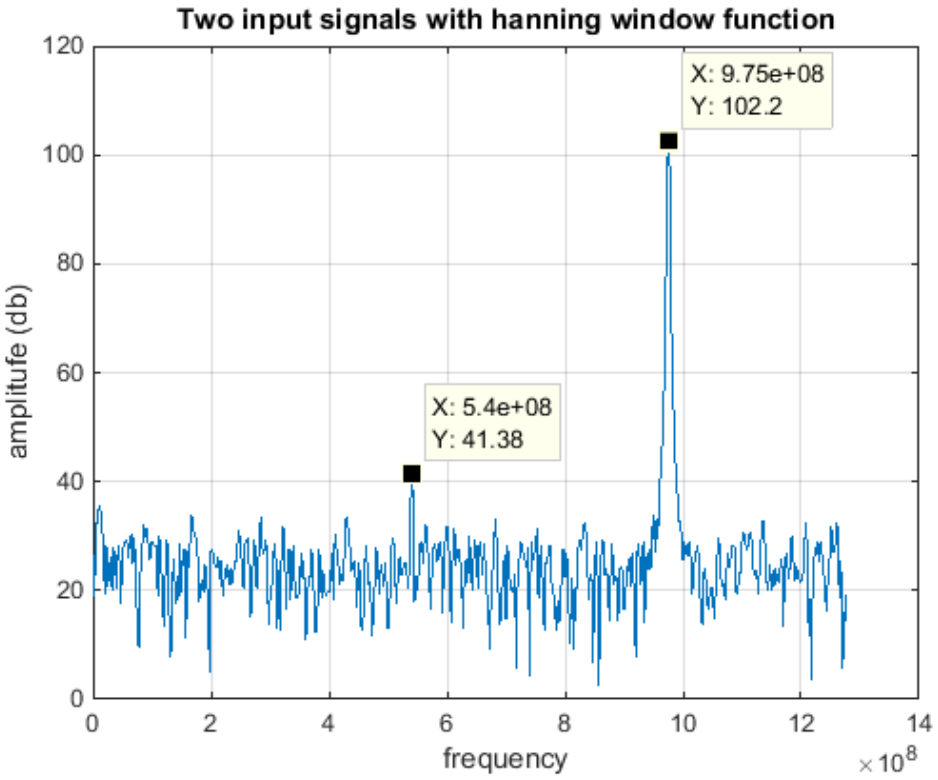

Fig 1.3.1 1024-point FFT Spectrum with Two Sine Wave Inputs

The stronger signal has a frequency of 975 MHz, and the other one has a frequency of 540 MHz. Noticing the main-lobe of the strong signal is as large as 10 bins away from the center bin. This, in turn, could mix up with the actual frequency of the small signal and generate false alarm which is undesired in the modern communication system. In this case, the super-resolution compensation method is applied to reduce the effect of the strong signal main-lobe and increase the possibility of accurately detecting the other signals. Fig 1.3.2 shows the flow of the super-compensation method.

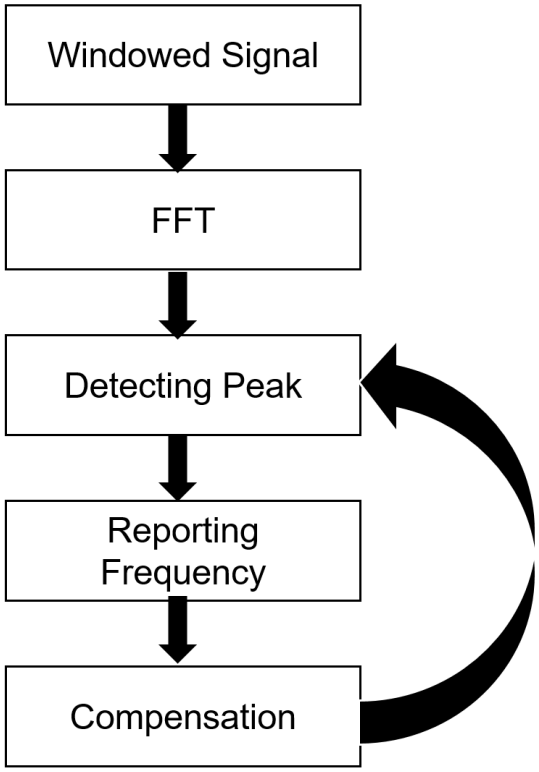

Fig 1.3.2 Super-compensation Flow

Ones the frequency f_1 of the strongest signal is found, then the f_1 frequency bin and other appropriate bins closed to the f_1 bin would be removed from the FFT spectrum to expose the actual second frequency bin. If more signals exist, repeat compensation to locate the more frequency bins. Fig 1.3.3 shows the compensation result comparing to Fig 1.3.1.

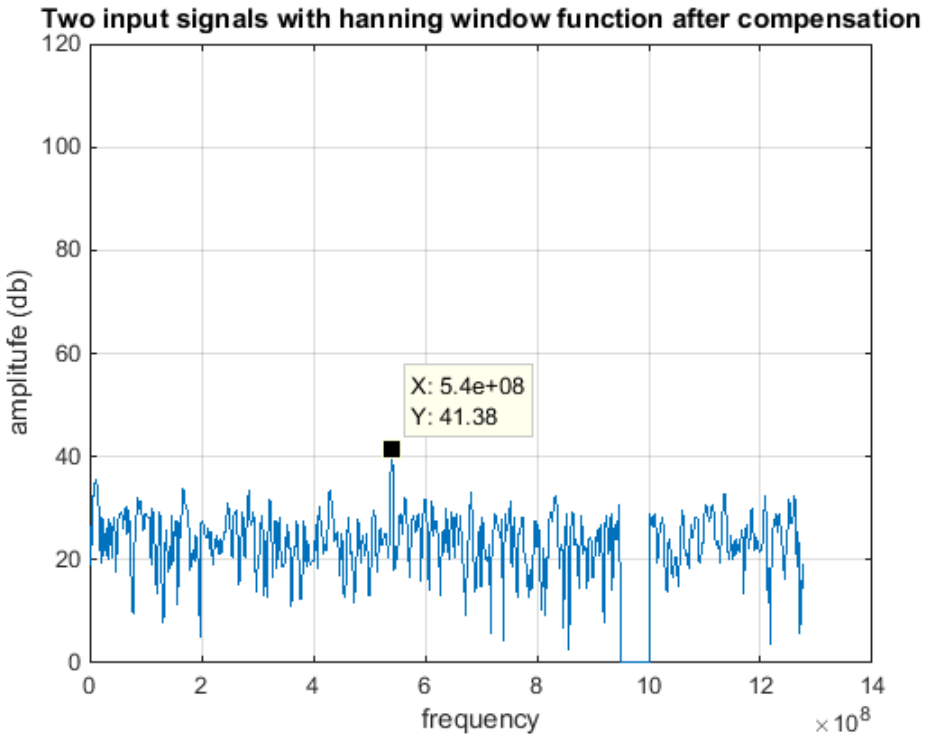

Fig 1.3.3 Compensation result of the two sine wave inputs

In the Fig 1.3.3, the actual second frequency bin is totally exposed by applying the compensation method. By using this super-resolution compensation method, as many as five signals could be detected simultaneous with an acceptable IDR [9].

1.4 Fine Frequency Estimation

Fine frequency estimation is an active way to speculate the accurate peak position from the frequency bins in FFT spectrum. By using the fine frequency estimation, the true frequency of the input signal could be extrapolated, and the limitation of the FFT frequency resolution is declined. Fig 1.4.1 shows an example of a FFT spectrum.

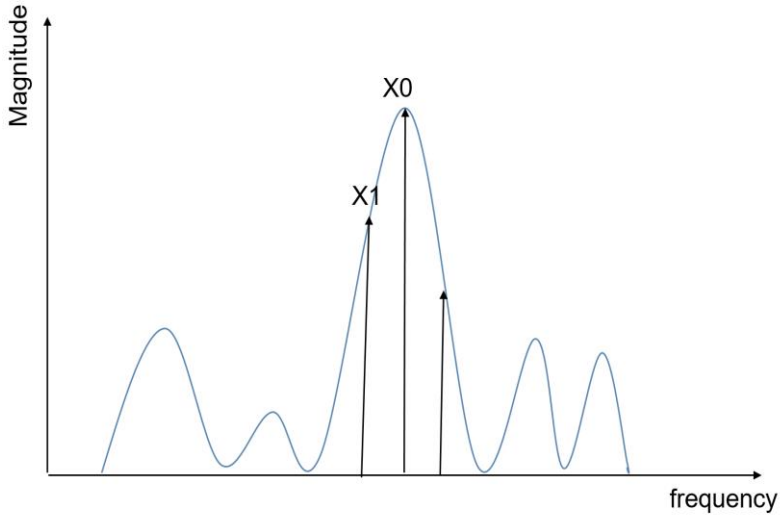

Fig 1.4.1 Frequency Response from FFT

Where X_0 is the peak of the data in the frequency domain and X_1 is the higher amplitude of two adjacent frequency bins. The equations of fine frequency estimation from various window functions are different. For example, if Fig 1.4.1 applies a hanning window from 1024-point FFT, the fine frequency estimation could be calculated by the following equations.

$$\mathrm{k} = \frac{2X_1 - X_0}{X_0 + X_1} \tag{1.4.1}$$

$$\mathrm{F} = (k_0 - 1 - k)2.5 \text{ MHz} \tag{1.4.2}$$

Where k_0 is the index of the X_0 and F is the adjusted frequency. 2.5 MHz is the resolution of the receiver in this thesis.

If X_1 is on the right side of the X_0 as shown in Fig 1.4.2, the adjusted frequency F is expressed as Eq. (1.4.3).

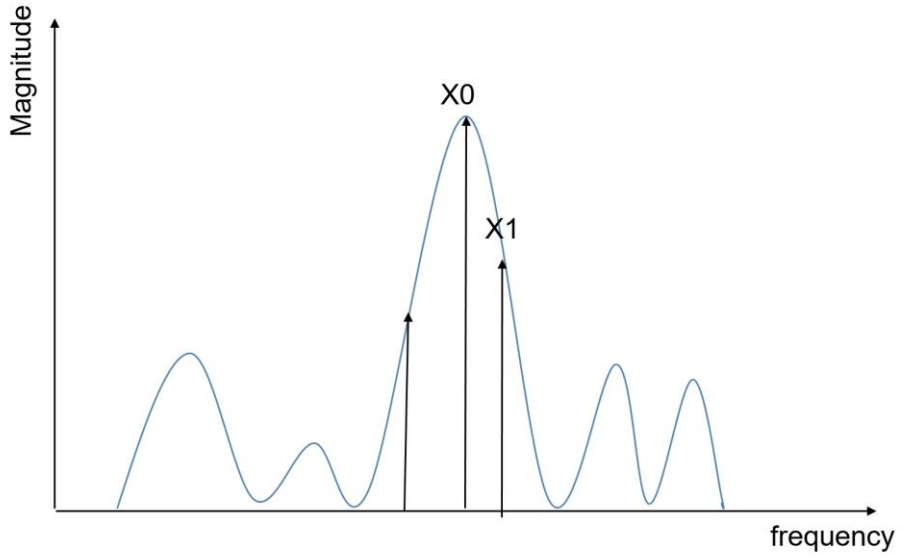

Fig 1.4.2 Frequency Response from FFT (case 2)

$$F = (k_0 - 1 + k)2.5 \text{ MHz} \quad (1.4.3)$$

In this thesis, the fine frequency estimation is introduced to the Hanning window with a different equation of the estimation, which is discussed in Chapter IV.

1.5 Two Signals Detection

As discussed in section 1.3, multiple signals detection capability is a critical evaluation index. The modern receivers still have a nice bit of challenge on performance of detecting multiple signals. Even the super-resolution compensation method is applied to the receiver system, which could highly improve the dynamic range and number of signals detection, the frequency resolution is still limited by the stronger signal due to its wide main-lobe. In case of the frequency of a weak signal closed to the frequency of a stronger signal, the frequency of the weaker signal would be removed by the super-resolution compensation method. Thus, the weaker could not be detected by the receiver system.

1.6 Motivation

With the incoming age of artificial intelligence and big data, electronic devices would be more intelligent, diversity and complexity. Development of receiver systems is a challenge that cannot be neglected.

In a FFT based receiver system, no matter how increase the point number of FFT or improve the performance of other components, signal resolution would always be limited by the main-lobe of the strong signal. In this case, a special block must be studied and applied to overcome this hard challenge.

1.7 Objective

The objective of this thesis is to implement a receiver system that can detect two signals which have close frequencies, then report the actual frequencies. The research about this thesis is simulated in the Matlab and Simulink.

1.8 Thesis Organization

The detailed organization of this thesis include:

- Chapter 1 gives the introduction of basic definitions and knowledge of the receiver system.
- Chapter 2 demonstrates the squarer and its function in the thesis.
- Chapter 3 shows the adaptive threshold technique for the receiver system to avoid false alarm.
- Chapter 4 discusses an algorithm to detect two signals and locate the actual frequency as precise as possible. Chapter 4 also shows the experimental result of this high frequency resolution wideband receiver system.

- Chapter 5 discusses the contribution of this research and future work to accomplish.

II. Squarer with Adaptive Gain

2.1 Squarer

Squarer is an irreplaceable hardware component in signal processing applications. It is widely used in multiplier, modulation, frequency division, filtering, vector quantization, image compression, pattern recognition, error correction, quantization, and signal power estimation [10]- [11], etc.

As squarer circuit design technology advances in size and power, it has become a critical component in ultra wideband (UWB) receivers. Fig 2.1.1 shows a basic type of UWB receiver block diagram. A squarer circuit is placed after the low noise amplifier (LNA) and a tunable gain to amplify the input signal, followed by an integrator tends to detect the power of the amplified signal [12].

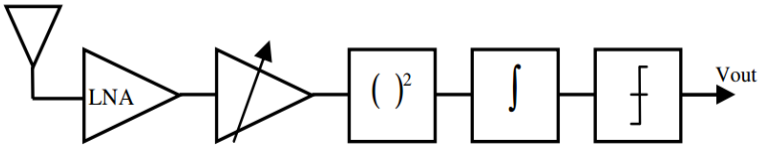

Fig 2.1.1 UWB Receiver Block

Another application of the squarer circuit is to double the frequency of input signal, which can be used in conjunction with FFT to accurately detect input signals and improve the dynamic range of the receiver [13]. Assume the input sinusoidal signal is expressed by the Eq. (2.1.1) with the amplitude -A,

The frequency ω, the phase angle θ and the additive white Gaussian noise (AWGN) n.

$$S = A\sin(\omega t + \theta) + n \tag{2.1.1}$$

After the squarer, the output is expressed as

$$S^2 = (A\sin(\omega t + \theta) + n)^2 \tag{2.1.2}$$

$$S^2 = A^2\sin(\omega t + \theta)^2 + 2nA\sin(\omega t + \theta) + n^2 \tag{2.1.3}$$

Using the double-angle formula in Eq. (2.1.4), the squared signal can be expressed in Eq. (2.1.5), which includes frequency components of 2ω and ω.

$$\cos 2x = 1 - 2\sin^2 x \tag{2.1.4}$$

$$S^2 = -\frac{1}{2}A^2\cos(2\omega t + 2\theta) + 2nA\sin(\omega t + \theta) + n^2 \tag{2.1.5}$$

The two frequencies of the squared signal, 2ω and ω, can be located in the FFT spectrum. Fig 2.1.2 shows the basic blocks of a receiver system with squarer.

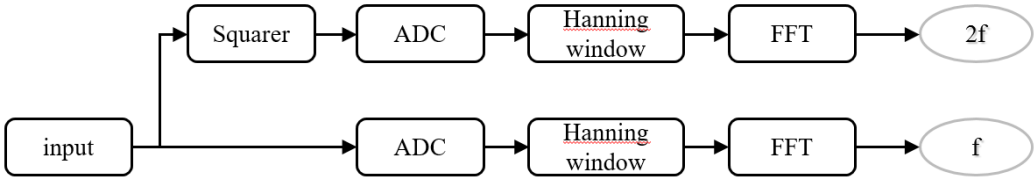

Fig 2.1.2 Basic Blocks of a Receiver System with Squarer

A 10-bit ADC used in this research is implemented by Simulink and has a dynamic range of -0.5V to 0.5V. This receiver system, after optimization for dynamic thresholding, can accurately locate f and 2f in a high dynamic range, which will be discussed in Chapter IV. Fig 2.1.3 and Fig 2.1.4 show the FFT responses of the non-squared input signal and squared signal.

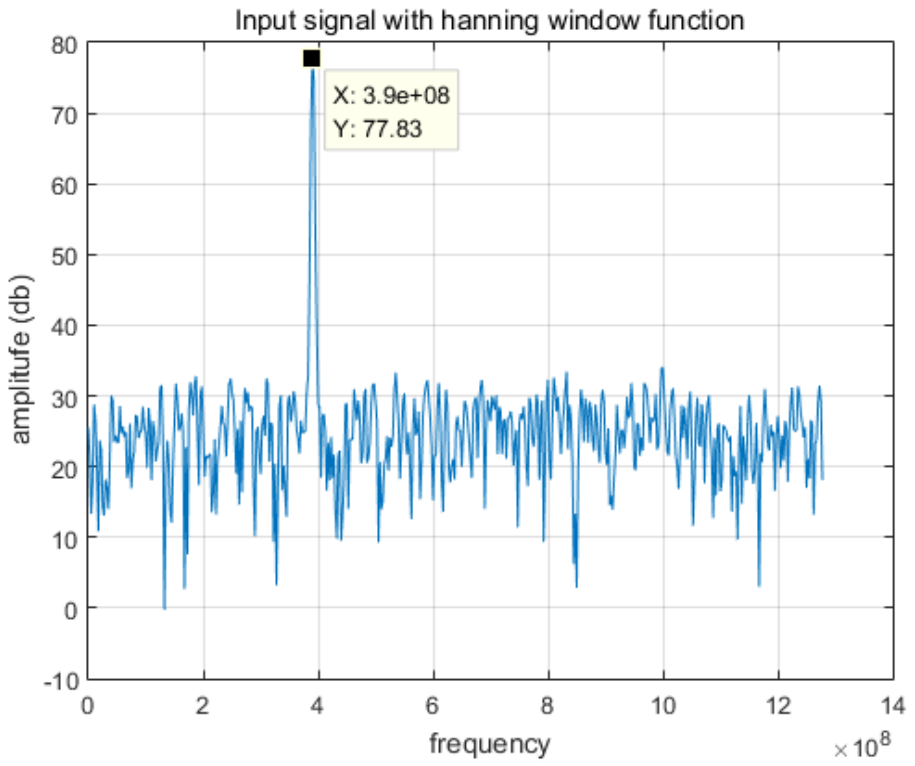

Fig 2.1.3 Non-squared Input Signal Frequency Response (f=390MHz)

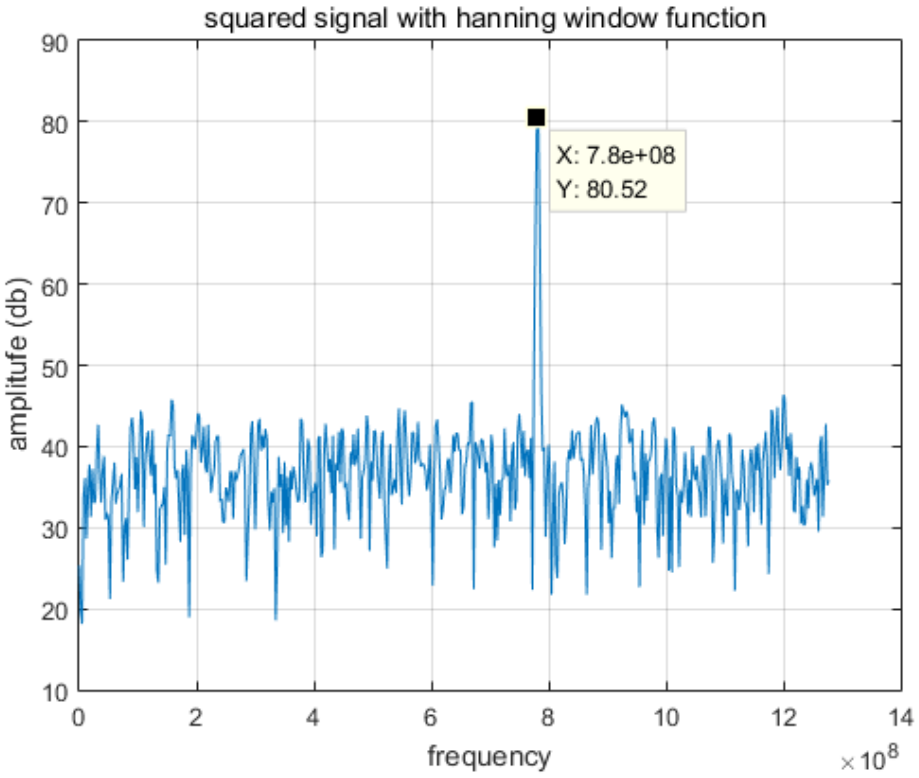

Fig 2.1.4 Squared Input Signal Frequency Response (2f=780MHz)

Note that the input frequency is 390 MHz, which is doubled to 780 MHz after the squared circuit in Fig 2.1.3. Since n is the white Gaussian noise, the second term $2n\mathrm{A}\sin(\omega\mathrm{t}+\theta)$ in Eq. (2.1.5) is small and will not cause false alarm after the receiver signal detection threshold is properly determined. So, only the 2f of the squared signal is detected in this case.

Considering two simultaneous signals ω_1 and ω_2, the input signal is expressed in Eq. (2.1.6).

$$\mathrm{S} = \mathrm{A}\sin(\omega_1 t + \theta_1) + \mathrm{B}\sin(\omega_2 t + \theta_2) + n \tag{2.1.6}$$

After the squarer, the output is expressed as

$$\mathrm{S}^2 = (\mathrm{A}\sin(\omega_1 t + \theta_1) + \mathrm{B}\sin(\omega_2 t + \theta_2) + n)^2 \tag{2.1.7}$$

$$= A^2\sin(\omega_1 t + \theta_1)^2 + 2A\mathrm{B}\sin(\omega_1 t + \theta_1)\sin(\omega_2 t + \theta_2) + B^2\sin(\omega_2 t + \theta_2)^2 + 2n\mathrm{A}\sin(\omega_1 t + \theta_1) + 2n\mathrm{B}\sin(\omega_2 t + \theta_2) + n^2 \tag{2.1.8}$$

The trigonometric sum and subtraction functions are expressed in Eq. (2.1.9) and Eq. (2.1.10).

$$\cos(\mathrm{x}+\mathrm{y}) = \cos x \cos y - \sin x \sin y \tag{2.1.9}$$

$$\cos(\mathrm{x}-\mathrm{y}) = \cos x \cos y + \sin x \sin y \tag{2.1.10}$$

Eq. (2.1.11) is obtained after using the above two equations.

$$\cos(\mathrm{x}-\mathrm{y}) - \cos(\mathrm{x}+\mathrm{y}) = 2\sin x \sin y \tag{2.1.11}$$

From Eqs. (2.1.4) and (2.1.11), the equation of the squared signals is expressed as

$$S^2 = -\frac{1}{2}A^2\cos(2\omega_1 + 2\theta_1) - \frac{1}{2}B^2\cos(2\omega_2 + 2\theta_2)$$

$$+ABcos[(\omega_1 - \omega_2)t + (\theta_1 - \theta_2)] - ABcos[(\omega_1 + \omega_2)t + (\theta_1 + \theta_2)]$$

$$+2nA\sin(\omega_1 t + \theta_1) + 2n\mathrm{B}\sin(\omega_2 t + \theta_2) + n^2 \tag{2.1.12}$$

The frequency components in the above equation are $2f_1$, $2f_2$, f_1+f_2, f_1-f_2, f_1 and f_2. As discussed in one signal case, $2nA\sin(\omega_1 t + \theta_1)$ and $2nB\sin(\omega_2 t + \theta_2)$ are small in comparison with other terms. Hence the total possible detectable frequency components after the squarer circuit could be $2f_1$, $2f_2$, f_1+f_2 and f_1-f_2. Figures 2.1.5 and 2.1.6 give FFT spectrum examples of two input signals after the squarer circuit.

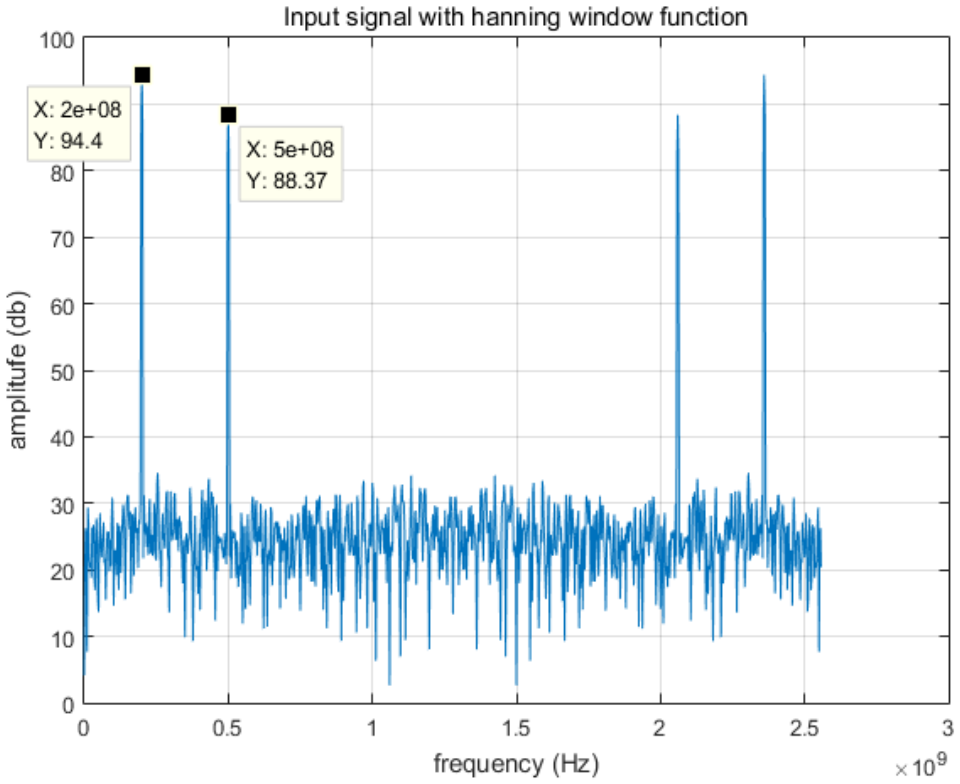

Fig 2.1.5 Two Input Signals Frequency Response (f1= 200MHz, f2=500MHZ)

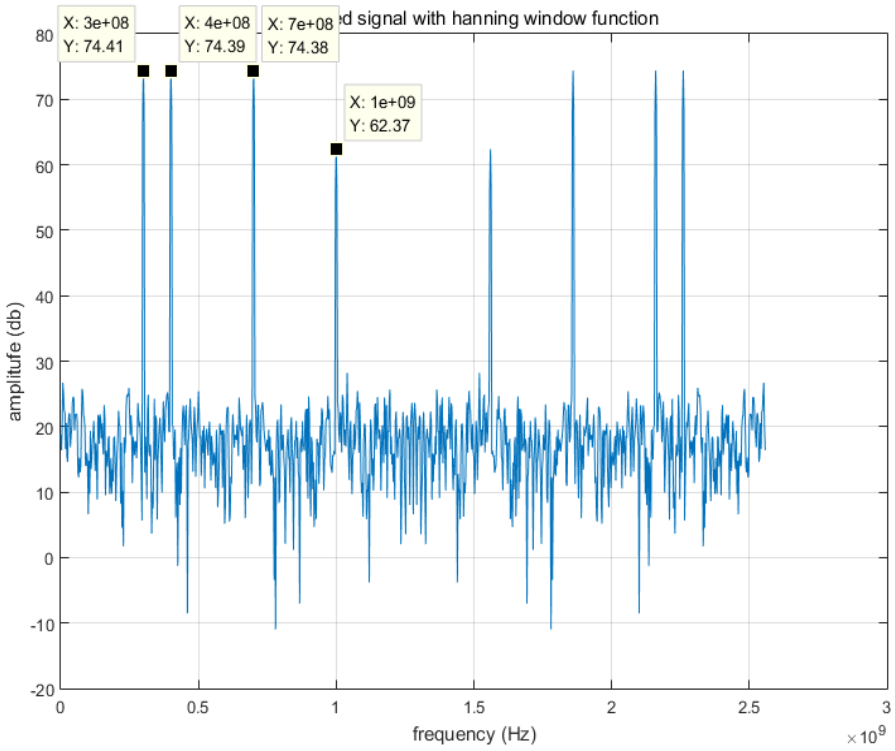

Fig 2.1.6 Squared Signals Frequency Response

Two signals are detected in Fig 2.1.5 with the two frequencies reported, $2*10^8$ Hz (f_1) and $5*10^8$ Hz (f_2). As shown in Fig. 2.1.6, the FFT spectrum of the squared signals reports four frequency components of 300 MHz (f_2-f_1), 400 MHz ($2f_1$), 700 MHz (f_2+f_1) and 1000 MHz ($2f_2$), which are consistent to the expression for S^2 shown in Eq. 2.1.12.

In this research, a high frequency resolution and dynamic range adaptive thresholding wideband receiver system is presented. It can accurately detect two simultaneous high dynamic range signals close to one frequency bin. The receiver design architecture and performance evaluation are presented. Another example of the squared signals in frequency domain is given in Fig. 2.1.7 and 2.1.8.

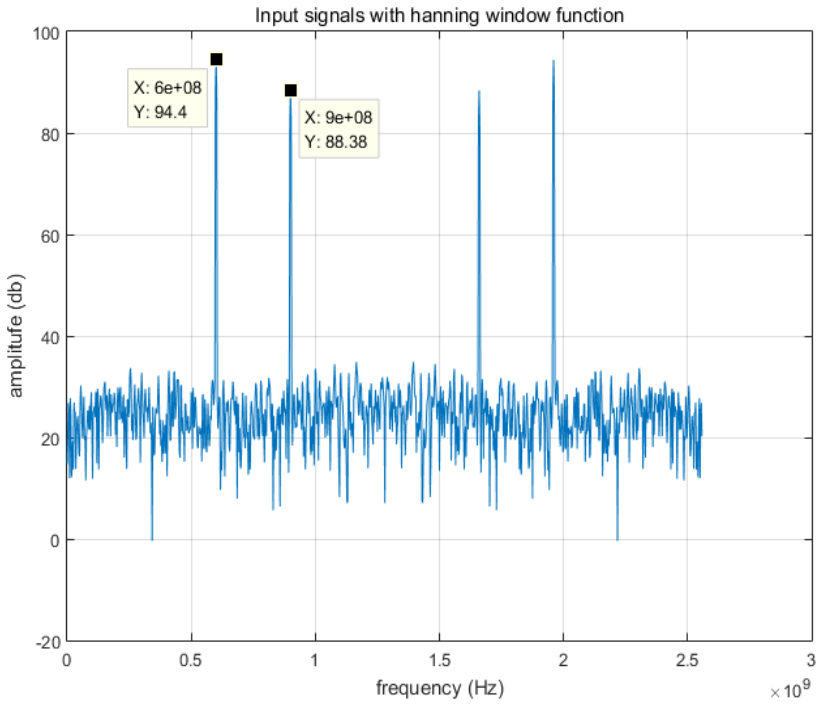

Fig 2.1.7 Two Input Signals with Frequency of 600MHz and 900MHz

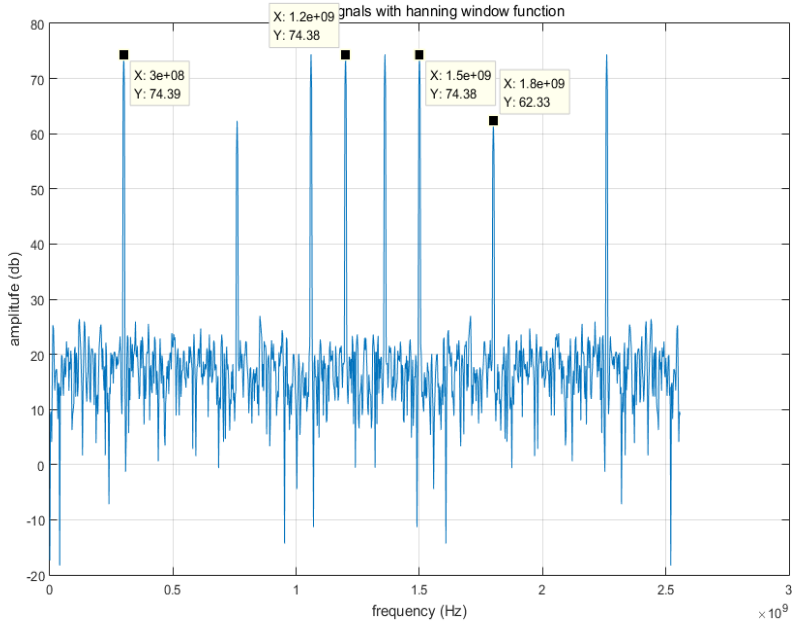

Fig 2.1.8 Squared Signals with Frequency of 600MHz and 900MHz

2.2 Adaptive Gain

Since the squared signal which has an amplitude $\frac{1}{2}A^2$, as discussed in Section 1.2, is much smaller than the original signal amplitude A when A << 1. The analog to digital converter (ADC) may not sample the squared signal accurately when an input signal amplitude is small and the squared amplitude $\frac{1}{2}A^2$ is less than the 1-b resolution of ADC. Fig. 2.2.1 and 2.2.2 give an example of two weak signals in the frequency domain.

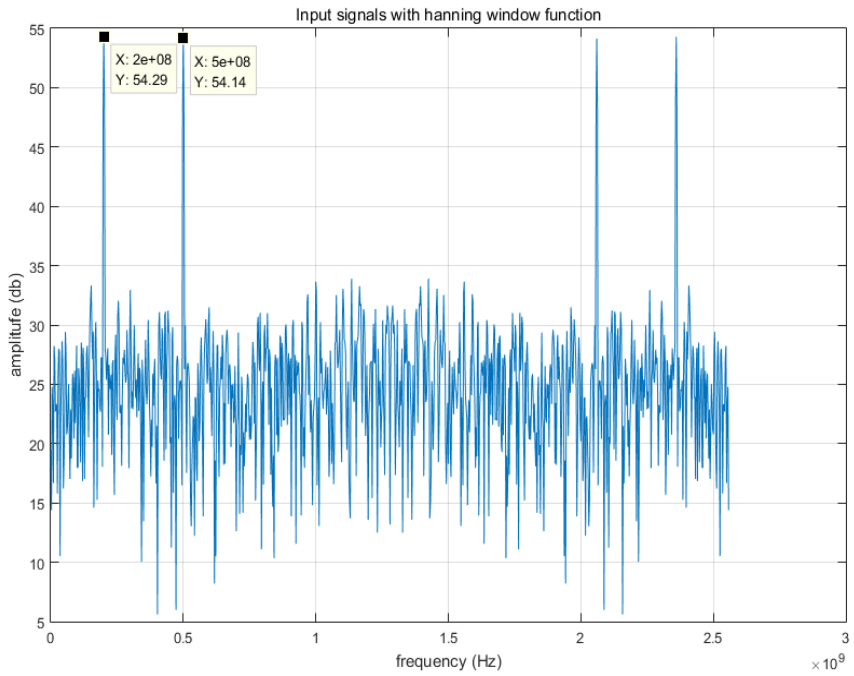

Fig 2.2.1 Two Weak Signals Frequency Response

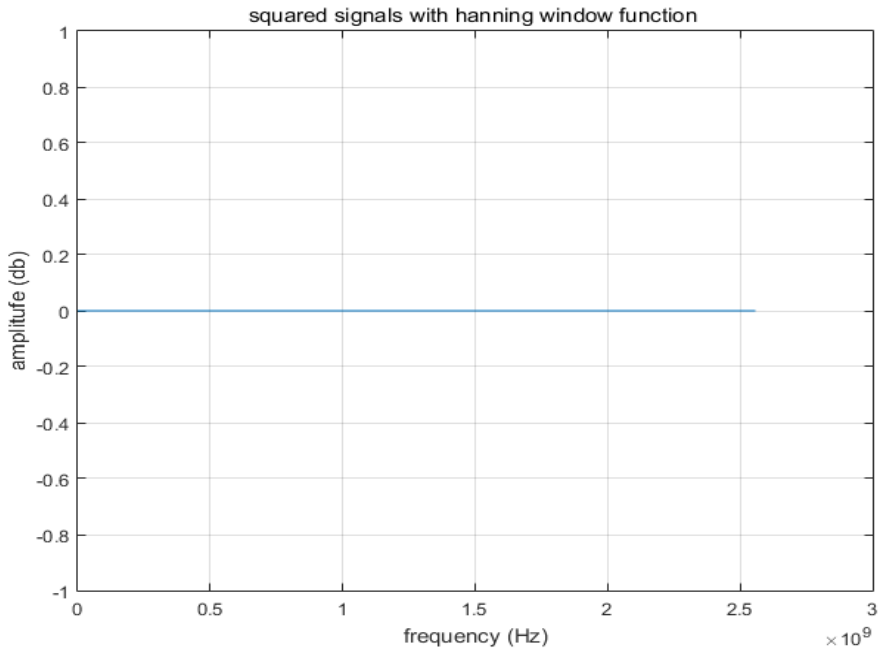

Fig 2.2.2 Squared Weak Signals Frequency Response

Both the two weak signals have small amplitude of 2 mV, which are sampled by a 10 bit ADC with a dynamic range from -0.5V to 0.5V. However, the squared amplitude, as small as 4 μV, cannot be sampled properly. Thus, Fig. 2.2.2 FFT squared spectrum does not shown any peak frequency.

In this case, a gain control amplifier is introduced to amplify the input signal before the signal is squared.

2.2.1 Amplitude Detection

It is worth noting that this amplifier gain is controllable because the amplitude summation of the input signals needs to be within the dynamic range of ADC. In order to set the controllable gain for different input amplitude, a peak detection block, detecting the amplitude value using the first several ADC sample data of incoming signals is introduced [14]. In this research, a 1024-point FFT is applied after the ADC block, thus, the peak detection block will detect the amplitude value of the first 1024

sampled data. After the amplitude evaluation, the amplifier gain is determined. Thereafter, the input signal will be amplified by the gain control amplifier before passing through the squarer circuit in the receiver system. Fig 2.2.3 shows the flow chart of adaptive gain control system.

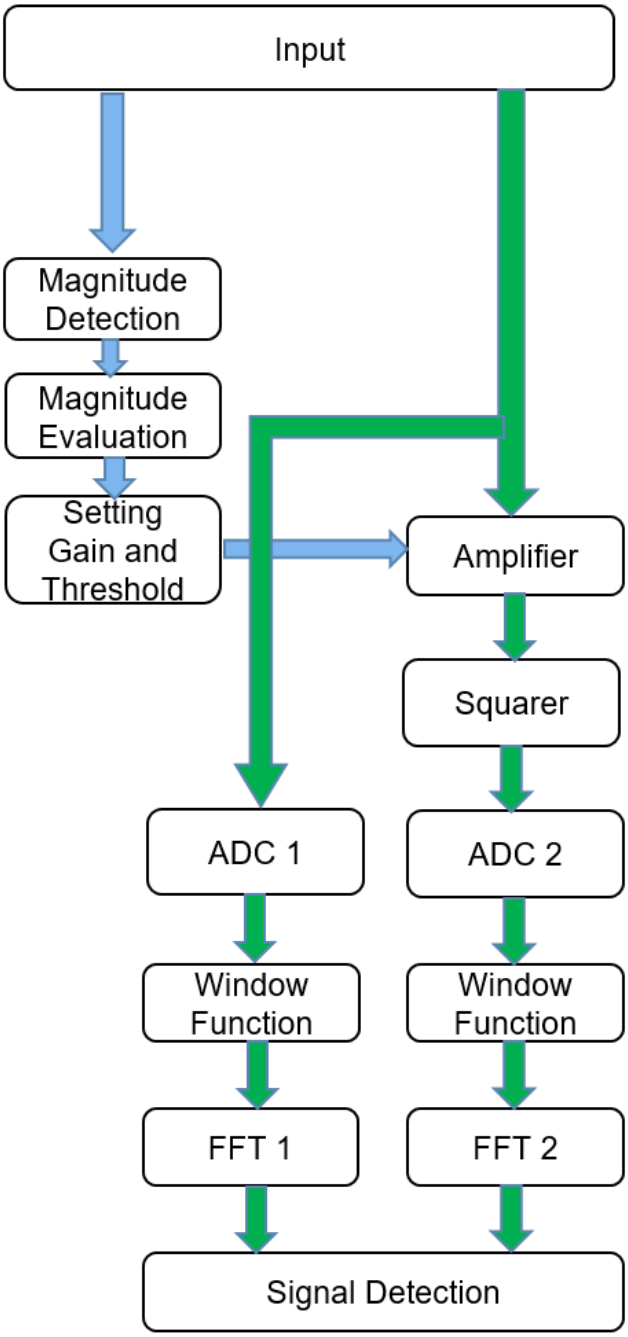

Fig 2.2.3 Flow Chart of Adaptive Gain Setting

2.2.2 Modulating Gain

Since the input data is sampled by the 10-bit ADC, the amplitude value range is from 0 to 1023. Five different gain values are applied to achieve a good sensitivity and dynamic range in this receiver system. Each gain based on different range of amplitude is determined by an amplitude evaluation block. Fig. 2.2.4 shows the flow chart of amplitude evaluation and gain setting.

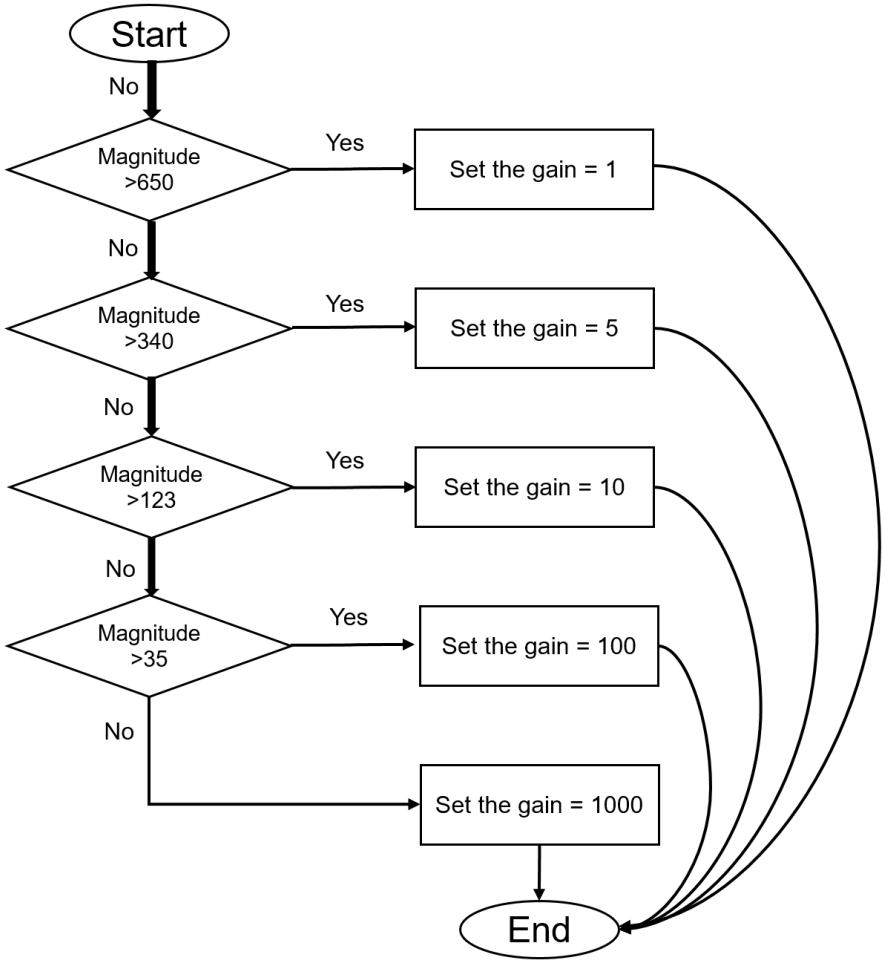

Fig 2.2.4 Flow Chart of Amplitude Evaluation and Gain Setting

After the first 1024 points input signal coming into the ADC, the peak amplitude is found before adjusting the amplifier gain. For example, two input signals in Fig. 2.2.1 have a peak amplitude of 2 mV, the amplitude summation value of this two input

signals is 13 after being sampled by the ADC. Then according to the flow chart the gain is set to 1000. The frequency response of the squared signal after the gain control 1000 amplifier is shown in Fig. 2.2.5.

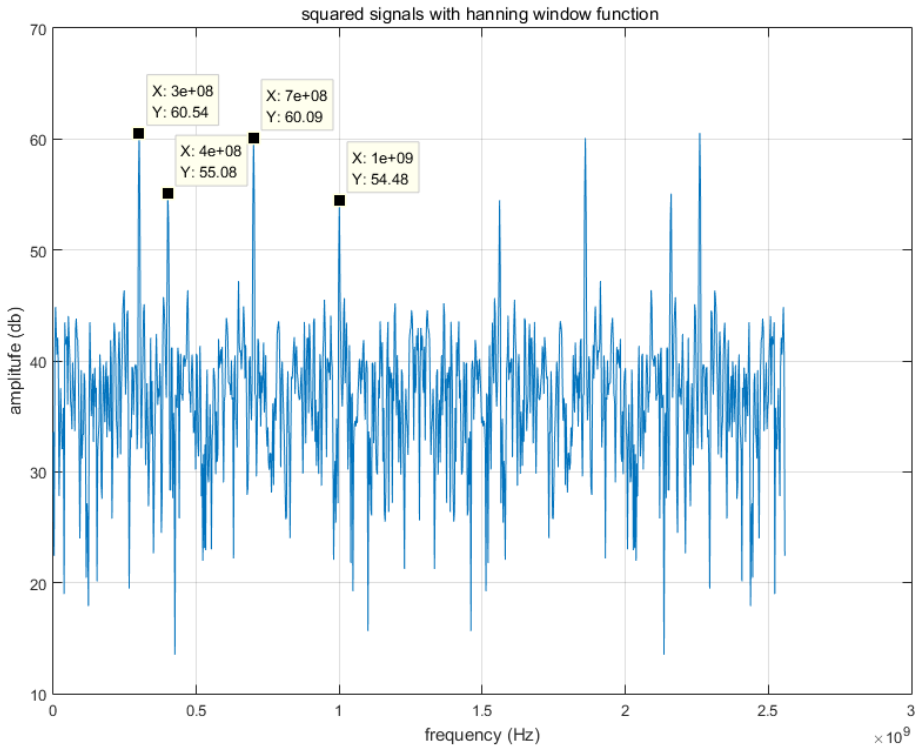

Fig 2.2.5 Amplified Squared Data in Frequency Domain (gain control = 1000)

In Fig 2.2.5, the frequency summation (f_1+f_2), frequency subtraction (f_2-f_1), double frequency of f_1 (f_1^2) and double frequency of f_2 (f_2^2) are all located in the FFT spectrum.

III. Adaptive Threshold

3.1 Threshold Setting for Non-squared Data

In order to report a signal from a FFT based receiver system, the maximum frequency bin corresponding to the signal must be found. In addition, the amplitude of this frequency bin has to be above a threshold which is determined based on the noise distribution and false alarm [15]. Thus, thresholding technique is a critical component in the receiver design that can affect receiver detection probability, false alarm rate and sensitivity.

In this research, the threshold for non-squared input data is determined by the noise Rayleigh distribution and false alarm rate of 10^{-7}. AWGN is introduced to evaluate noise effect and determine the threshold. This standard deviation is determined by 1 bit resolution of the ADC. Fig 3.1.1 shows the flow chart of noise distribution evaluation.

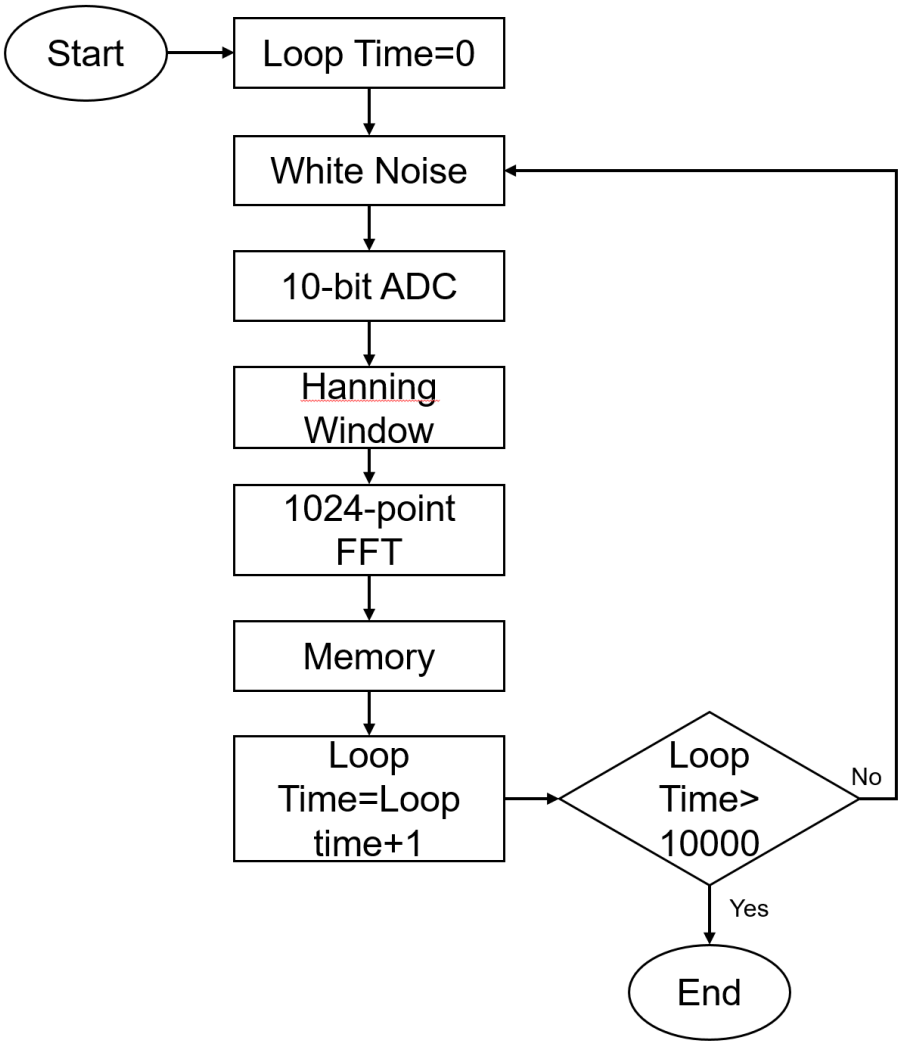

Fig 3.1.1 Noise Distribution Evaluation.

In the above evaluation flow, the total 10,240,000 sampled data points, which is 10,000 frames of 1,024-point FFT, are collected and stored in frequency domain by using FFT. Theoretically, the distribution of white noise data in frequency domain is a Rayleigh distribution. The x-axis value within around 10^{-7} of the total area of the distribution figure from right to left is selected as the threshold, which gives a false alarm rate of 10^{-7} when there is no incoming signal except noise. Fig 3.1.2 shows the distribution form of white noise.

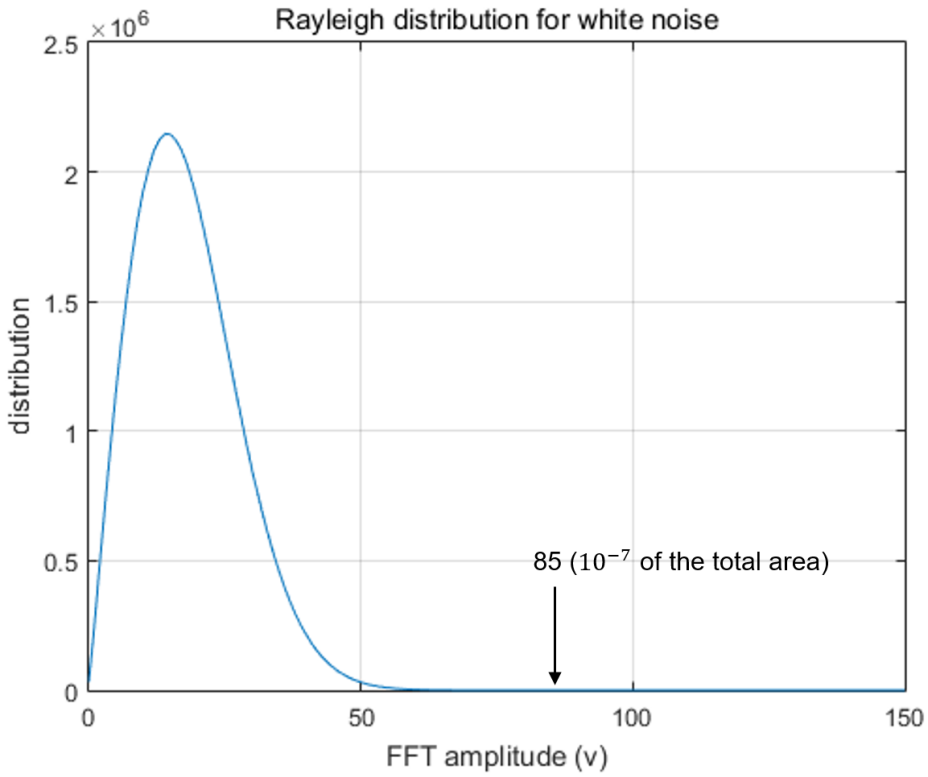

Fig 3.1.2 AWGN Rayleigh Distribution

By calculating the area of the distribution, the threshold is set to 85 Volts or 39 dBm in frequency domain. Using this threshold value Table 3.1.1 shows the

sensitivity table for single signal detection. In this case, the receiver sensitivity is close to -10 dB of SNR where 90% detection rate is achieved. Table 3.1.1 shows the sensitivity for single signal detection.

Table 3.1.1 Sensitivity of Single Signal

SNR	-11	-10.5	-10	-9.5	-9	-8.5	-8
Detection Rate (%)	80.3	84.57	92.34	96.76	98.94	100	100

Fig 3.1.3 gives an example of one signal 1040 MHz of -10 dB SNR in frequency domain. The maximum amplitude in this figure is greater than the threshold of the non-squared data, thus, the frequency of this input signal is detected.

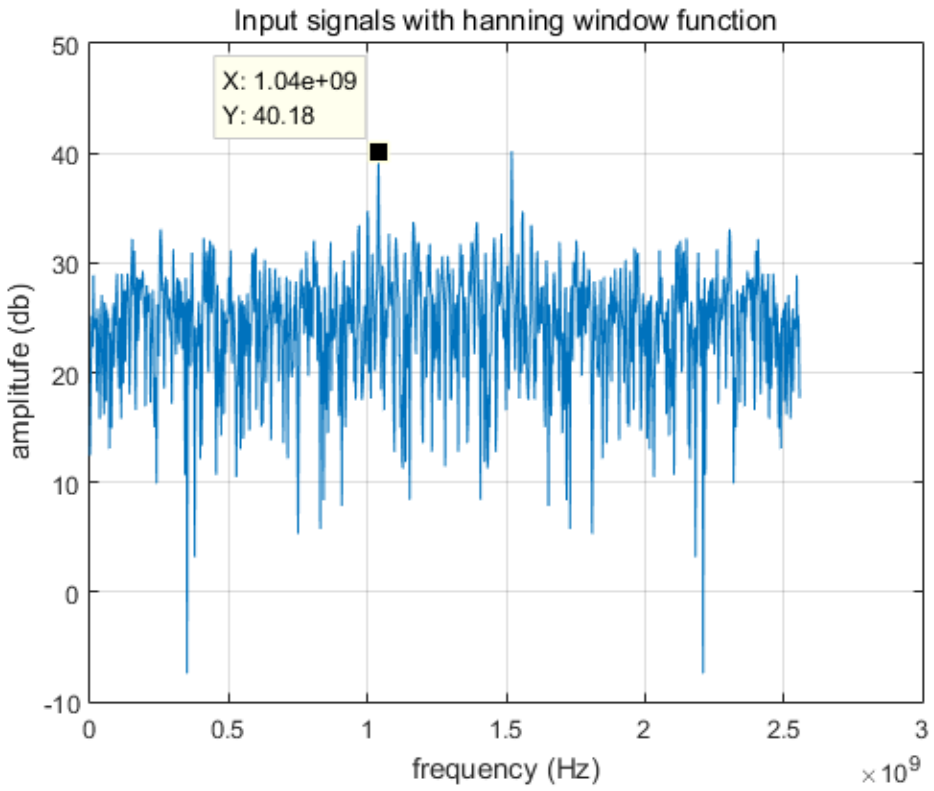

Fig 3.1.3 Single Signal of -10 SNR in Frequency Domain.

Ideally, dual threshold can be applied to the non-squared input data to increase the dynamic range when there are multiple input signals to the receiver system [16]. In this research, dual thresholds technique for non-squared data is necessary to be applied after the practical simulation base on the threshold 39. Fig 3.1.4 shows an example of two signal inputs in frequency domain.

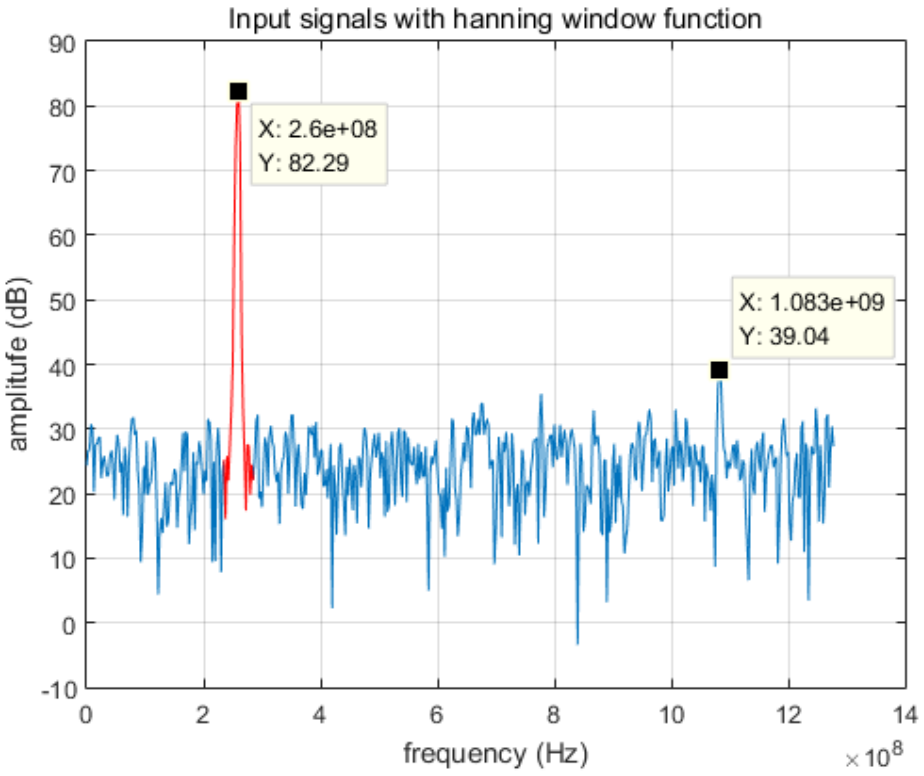

Fig 3.1.4 Two Signals of 259.67MHz and 255.97 MHz in Frequency Domain.

It is worth noting that the frequencies of the weak signal and strong signal are close to each other and a spur arises (i.e. 39.04 dB) which is above the threshold 39 dB. In this case, dual threshold has to be applied. After practice simulation, setting the second threshold to 40 dB could avoid false alarm.

3.2 Adaptive Threshold for Squared Data

Because multiple frequency peaks are to be detected for squared data in FFT spectrum as discussed in section 2.1, false alarms could occur due to multiple signal interference. Meanwhile, strong signals would generate wide main-lobes and side-lobes and therefore, increase interferences so as to miss weak signal detection or cause false alarms. In this case, using the fixed threshold technique, the given receiver would not detect weak signals and thus, reduce two-signal dynamic range. Modern elaborate receiver system is required to be more accurate and have a high dynamic range, therefore, modulating and determining an optimal.

The adaptive thresholding technique proposed in this research will resolve these problems.

3.2.1 Threshold Measurement

To set an appropriate threshold for the squared data, the noise floor must be measured.

From the Eq. 2.1.12, magnitudes of 2f are $\frac{1}{2}A^2$ and $\frac{1}{2}B^2$, amplitude of f_1-f_2 and f_1+f_2 is AB. Generally, comparing to the 2f, the f_1-f_2 and f_1+f_2 are helpful in detecting input signals, which will be discussed in Chapter 4. Thus, making both f_1-f_2 and f_1+f_2 detectable without causing false alarm is a key requirement for adaptive thresholding. Considering two high dynamic range signals, one strong (amplitude A) and one weak (amplitude B), if AxB is small then both f_1-f_2 and f_1+f_2 would be difficult to detect. So two high dynamic range signals are considered in adaptive thresholding technique. If the weak signal amplitude B is very small, then the amplitude of the double frequency of this weak signal (B^2) is too small. Therefore, the double frequency signal cannot be

detected. Fig 3.2.1 gives an example for a strong signal and a weak signal in frequency domain. Fig 3.2.2 shows frequency response for the same data but be squared.

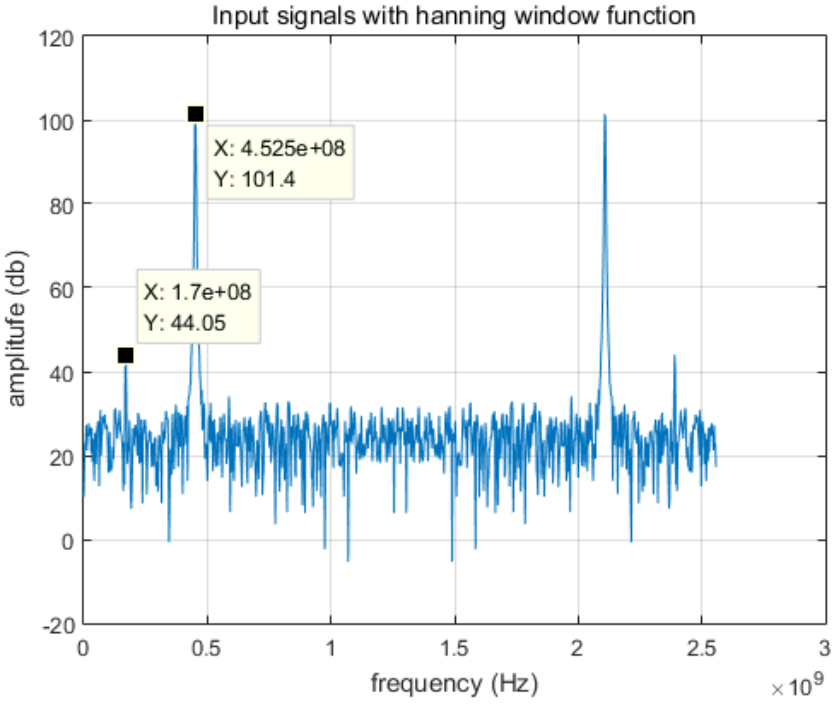

Fig 3.2.1 Non-squared Strong and Weak inputs in Frequency Domain

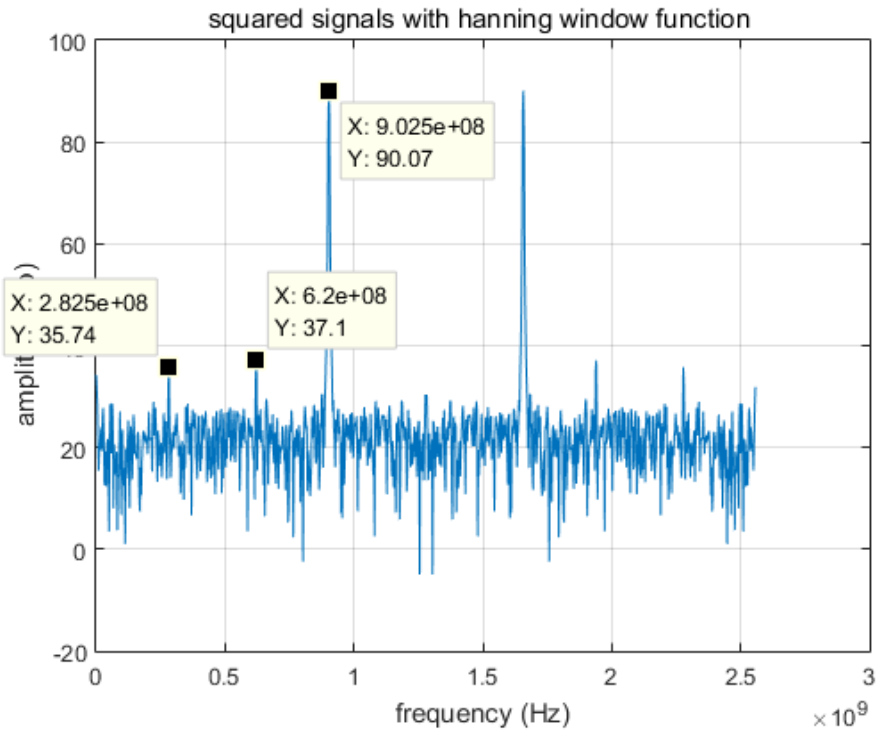

Fig 3.2. 2 Squared Strong and Weak Inputs in Frequency Domain

Suppose the frequency of the strong signal is f_1 which is 452.5M Hz, and the frequency of weak signal is f_2 which is $1.7*10^8$ Hz. Then the $2f_1$ (902.5 MHz), f_1-f_2 (282.5 MHz) and f_1+f_2 (620 MHz) are determined in the second FFT spectrum where the reported frequency of f_1 is 451.5 MHz and f_2 is 169.5 MHz.

In order to achieve a dynamic range for this receiver system, the strong signal and weak signal must be swept from a wide range of amplitudes. By simulating in Matlab and Simulink, the weak signal should have at least -6.5 dB SNR to avoid false alarm, and the strong signal has to be at least 6.5 SNR to achieve a 90% signal detection for $2f_1$, $2f_2$, f_1-f_2 and f_1+f_2.

The following tables based on 5 different gains for squared data, which is discussed in section 2.2.2, give the results of the simulation for different signal

amplitudes. Each case collects 102,400,000 (>10^8) points data to inspect the threshold for a false alarm rate of 10^{-7}.

Table 3.2.1 Thresholds for Squared Data with a Controllable Gain of 1000

Weak Signal SNR	Strong Signal SNR	Maximum Amplitude for non-squared data after ADC	Minimum Amplitude for non-squared data after ADC	Mean Amplitude or non-squared data after ADC	Detection Probability	Threshold
-7	6.5	15	10	12	84.83	51.7
-6.5	6.5	15	10	12	90.97	51.8
-6.5	7	16	10	13	90.86	52.4
					93.49	52.1
-6.5	7.5	16	10	13	90.08	53
					93.74	52.6
-6.5	8	17	10	13	90.38	53.5
					96.45	52.6
-6.5	8.5	17	11	14	90.16	54
					96.06	53.2
-6.5	9	18	11	14	89.82	54.5
					95	53.9
-6.5	9.5	18	12	15	90.38	54.9
					94.52	54.4
-6.5	10	18	12	15	90.55	55.5
					96.22	54.7
-6.5	10.5	19	12	16	90.42	55.9
					96.63	55
-6.5	11	19	12	16	89.79	56.5
					95.44	55.8
-6.5	11.5	20	14	17	90	57
					97.17	55.9
-6.5	12	21	14	17	89.86	57.5
					95.97	56.7
-6.5	12.5	21	15	18	90.57	57.9
					94.73	57.4
-6.5	13	22	15	19	90.33	58.5
					96.81	57.5
-6.5	14	24	16	20	89.7	59.5
					97.5	58.2
-6.5	15	26	17	22	90.52	60.5
					96.93	59.5
-6.5	16	28	19	24	90.03	61.5
					97.45	60.3

-6.5	17	29	21	26	90.28	62.5
					97.19	61.4
-6.5	18	32	23	28	90.5	63.5
					97.57	62.3
-6.5	19	34	24	31	90	64.5
					97.14	63.4
-6.5	20	38	28	34	90.2	65.5
					97.64	64.2
-6.5	21	41	30	37	90.29	66.5
					97.43	65.3
-6.5	22	45	33	41	90.3	67.3
					97	66

Table 3.2.2 Thresholds for Squared Data with a Controllable Gain of 100

Weak Signal SNR	Strong Signal SNR	Maximum Amplitude for non-squared data after ADC	Minimum Amplitude for non-squared data after ADC	Mean Amplitude or non-squared data after ADC	Detection Probability	Threshold
-6.5	20	38	28	33	90.2	45.7
					96	44.6
-6.5	21	41	30	37	90.13	47.1
					93.45	46.1
-6.5	22	45	33	41	90.23	47.5
					97.58	46.2
-6.5	23	49	36	45	90.47	48.4
					95.8	47.6
-6.5	24	54	40	50	90.57	49.4
					97.15	48
-6.5	25	59	42	55	90.68	50.4
					96.66	49.3
-6.5	26	66	49	61	90.6	51.4
					96.57	50.3
-6.5	27	72	56	68	90.37	52.4
					96.56	51.3
-6.5	28	80	60	76	90.47	53.4
					97	52.1
-6.5	29	89	65	85	90.67	54.4
					97.08	53
-6.5	30	98	73	94	90.54	55.4
					94.38	54.9
-6.5	31	109	78	105	90.67	56.4
					97.12	55

-6.5	32	122	92	117	89.67	57.5
					96.38	56.4
-6.5	33	136	97	131	90.75	58.6
					96.58	57.4
-6.5	34	150	117	146	90.5	59.3
					97.15	58

Table 3.2.3 Thresholds for Squared Data with a Controllable Gain of 10

Weak Signal SNR	Strong Signal SNR	Maximum Amplitude for non-squared data after ADC	Minimum Amplitude for non-squared data after ADC	Mean Amplitude or non-squared data after ADC	Detection Probability	Threshold
-6.5	33	136	97	131	90	38.4
					95.26	37.7
-6.5	34	150	117	146	90.39	39.4
					95.66	38.6
-6.5	35	168	124	164	90.58	40.4
					96.55	39.4
-6.5	36	188	140	183	90.41	41.4
					95.3	40.7
-6.5	37	209	159	205	90.55	42.4
					96.49	41.4
-6.5	38	233	178	229	89.5	43.5
					94.54	42.9
-6.5	39	261	198	257	90.6	44.4
					97.26	43
-6.5	40	292	226	287	90.59	45.4
					96.71	44.3
-6.5	41	327	253	322	90.57	46.4
					97.14	45
-6.5	42	365	272	360	90.56	47.4
					97	46.1
-6.5	43	409	310	404	90.57	48.4
					95.76	47.6

Table 3.2.4 Thresholds for Squared Data with a Controllable Gain of 5

Weak Signal SNR	Strong Signal SNR	Maximum Amplitude for non-squared data after ADC	Minimum Amplitude for non-squared data after ADC	Mean Amplitude or non-squared data after ADC	Detection Probability	Threshold
-6.5	42	365	272	360	90.1	41.5
					96.51	40.3
-6.5	43	409	310	404	90.02	42.4
					96.36	41.4
-6.5	44	457	359	453	90.15	43.4
					96.42	42.3
-6.5	45	512	399	507	90.29	44.4
					95.35	43.7
-6.5	46	574	419	568	89.84	45.4
					95.64	44.5
-6.5	47	644	471	638	90.01	46.4
					95.96	45.3

Table 3.2. 5 Thresholds for Squared Data with a Controllable Gain of 1

Weak Signal SNR	Strong Signal SNR	Maximum Amplitude for non-squared data after ADC	Minimum Amplitude for non-squared data after ADC	Mean Amplitude or non-squared data after ADC	Detection Probability	Threshold
−6.5	48	719	556	715	82.65	33.8
−6.5	49	806	613	802	89.34	34.3
−6.5	50	903	670	899	89.53	35.3
−6.5	51	1013	730	1008	63.27	37.6

The weak signals is fixed where the strong signals have a SNR from 6.5 to 51 dB. Each strong signal has two thresholds in the above tables. By using the first threshold, around 90% probability detection is achieved. By using the second threshold there is no false alarm. In order to get a high dynamic range, the second threshold would be used as the squared data threshold.

It is worthy noting that some strong signals such as 33 SNR, 34 SNR are both listed in Table 3.2.2 and Table 3.2.3 but have different thresholds. A reason of this is the inputs with same SNR could have different gain for squared data. For example, if the SNR of the amplitude summation of the input signals is 34, the amplitude for non-squared data could be any value from 117 to 150 after sampling by ADC, so the gain evaluation block can adjust the amplifier gain to 1000 or 100 by comparing the amplitude with 123 which was set in Chapter II. Thus, the strong signal with 34 dB SNR are both tested and analyzed with the control gain of 1000 and 100.

3.2.2 Threshold Modulation

After the appropriate thresholds are obtained, a final threshold table is built to modulate the final threshold for squared data. To apply the adaptive threshold, the amplitude detection technique as discussed in section 2.2.1 is introduced to adjust the threshold corresponding to the threshold table. Fig 3.2.3 shows the flow chart for the threshold modulation.

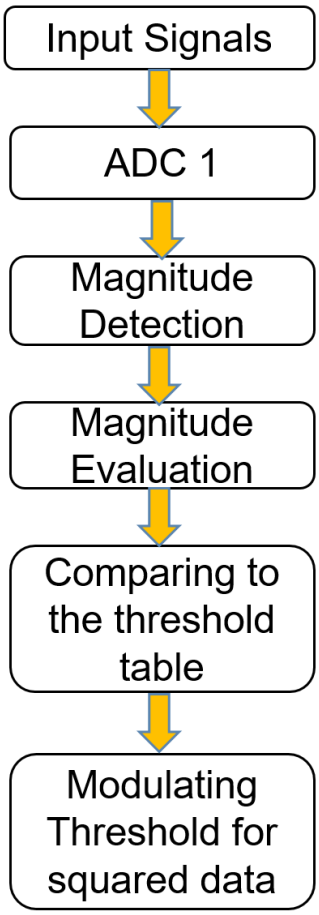

Fig 3.2.3 Flow Chart for the Threshold Modulation

IV. Two Signals Detection

4.1 Detecting the First Signal.

The basic idea of detecting the first signal is using a 1,024 points FFT with a window function to transfer the data from time domain to frequency domain. When input signal coming into the receiver system, the data would be sampled by ADC and be stored in memory. Note that the DC effect is removed by subtracting the average value of the sampled data. Besides, in order to reduce the effect of side-lobe, window function is applied in the time domain before the FFT analysis. At last, the frequency bin which has a maximum amplitude and are above the threshold represent the strongest amplitude of input signals. Fig 4.1.1 shows the flow chart of the first signal detection and Fig 4.1.2 gives an example for FFT spectrum.

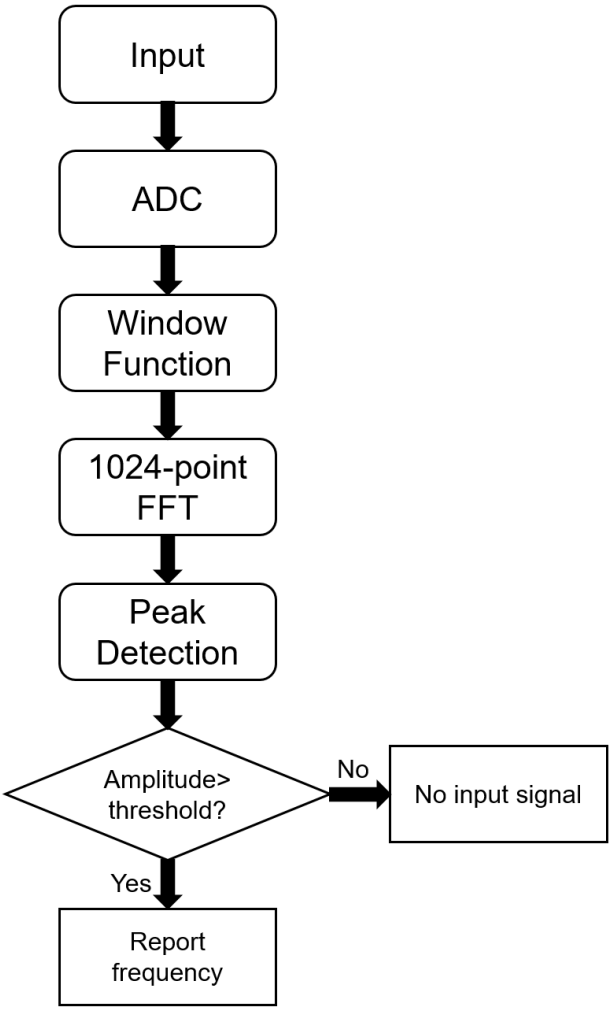

Fig 4.1.1 Flow Chart for Detecting the First Signal

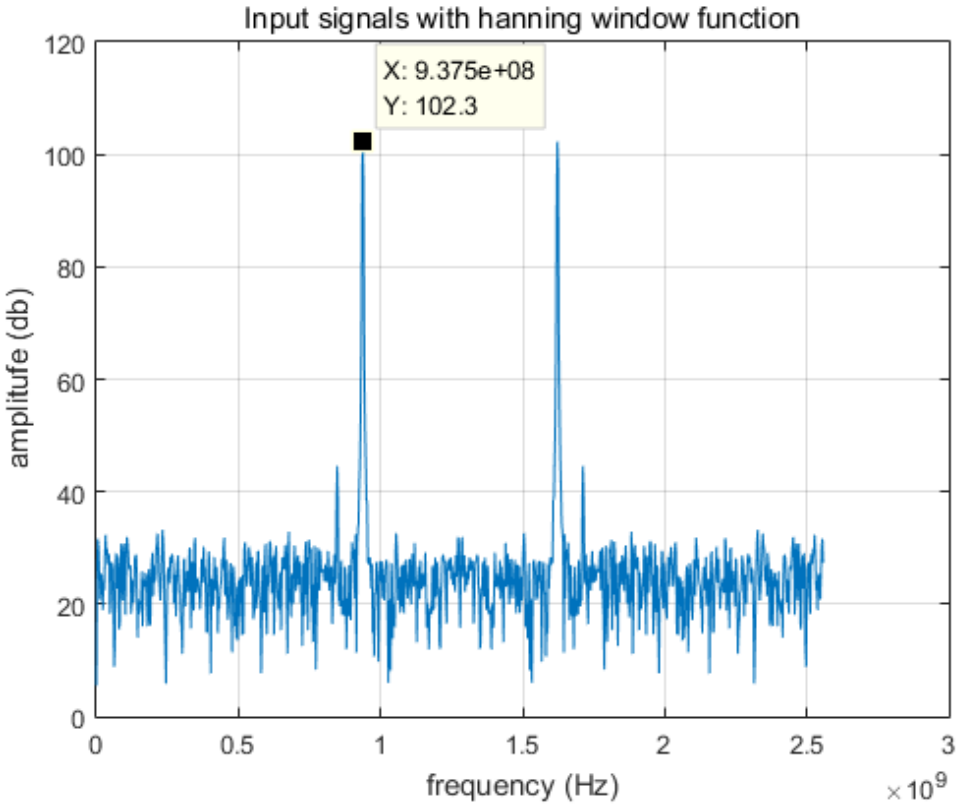

Fig 4.1.2 Maximum Amplitude in Frequency Domain

4.2 Fine Frequency Estimation

As discussed in section 1.4, fine frequency estimation can be applied to improve the frequency resolution. Two examples are given in Fig 4.2.1 and Fig 4.2.2.

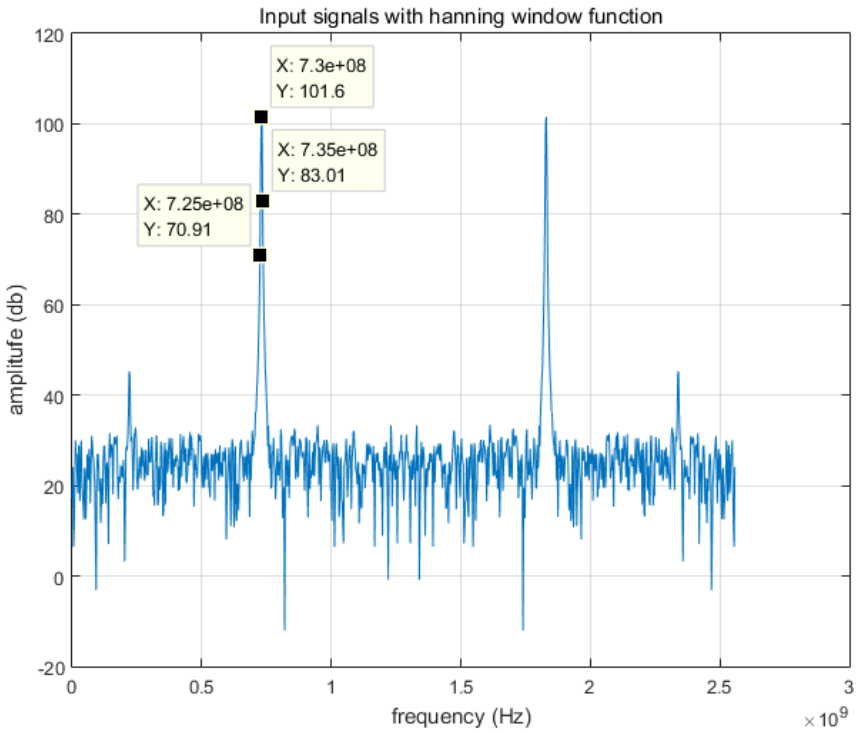

Fig 4.2.1 Right Side Fine Frequency Estimation

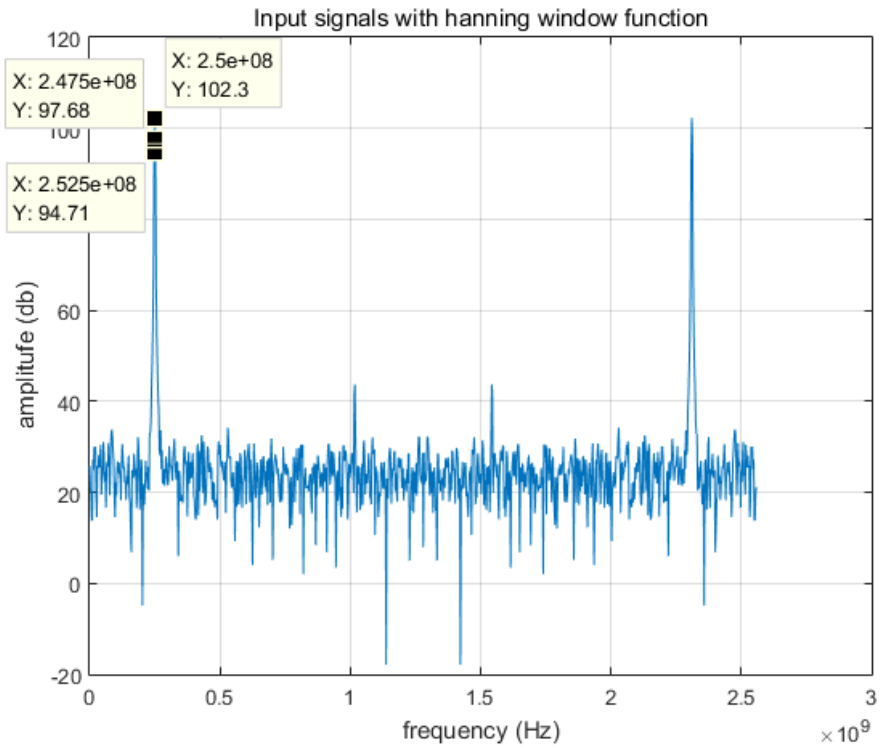

Fig 4.2.2 Left Side Fine Frequency Estimation

Based on the analysis of the Fig 4.2.1, the frequency of the first signal is located at 730 MHz, and the actual frequency of this signal is 730.93 MHz. Noticing the right bin has a higher amplitude than the left bin, Eq. (1.4.2) can be applied to estimate the actual frequency. Substitute 101.6 to X_0 and 83.1 to X_1, the adjusted frequency is calculated to be 730.87 MHz, which is closer to the actual frequency. Fig 4.2.2 can be estimated by Eq. (1.4.3) due to the left side bin has a higher amplitude than the right side bin, where the adjusted frequency is 248.84 MHz and the actual frequency is 249.72 MHz.

4.3 Detecting the Second Signal

Detecting the second signals with high dynamic range and high frequency resolution is quite a challenging in modern wideband digital receiver due to the effect of the main-lobe and side-lobe created by the strong signal. To solve the problem, a squarer circuit and an algorithm for determining the frequency of the second signal are discussed in this section.

4.3.1 Determining the Existence of the Second Signal

To detect multiple signals by FFT analysis, a compensation method has been presented to remove the main-lobe, side-lobes and spurs of the strong signal. Then the next maximum amplitude frequency bin is exposed. Fig 4.3.1 and Fig 4.3.2 give an example for the result of the compensation method.

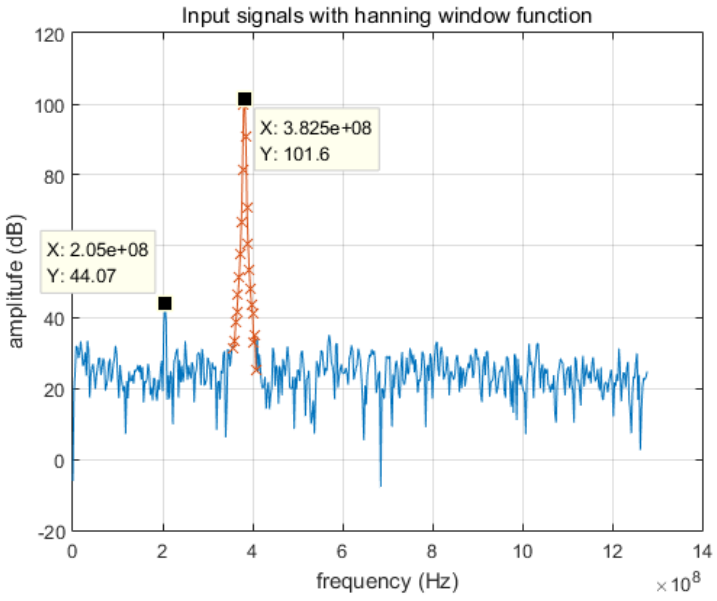

Fig 4.3.1 FFT Spectrum without Compensation

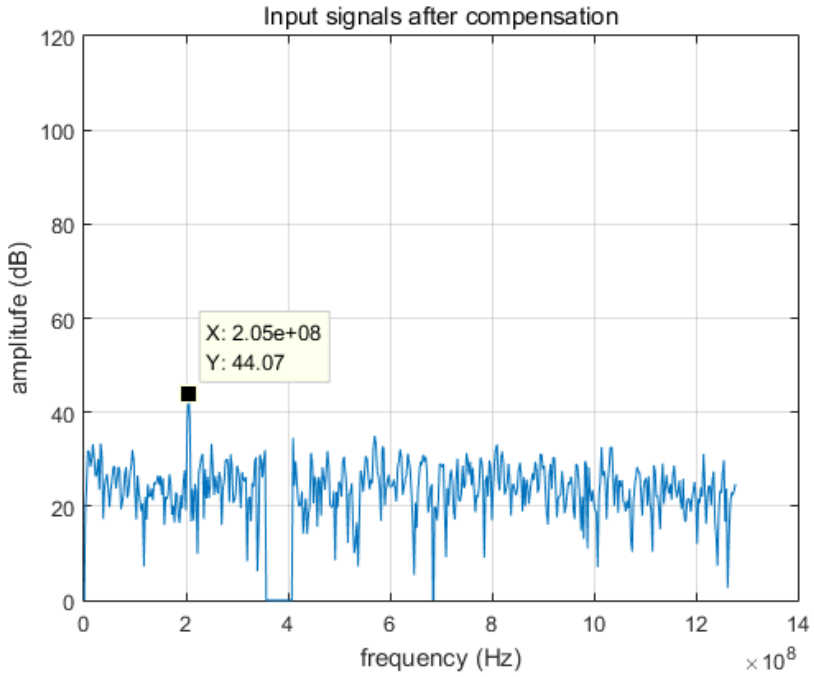

Fig 4.3.2 FFT Spectrum with Compensation

From the above figures, it is worthy noting that there are as many as 20 frequency bins in the main-lobe of the strong signal. The second signal in these frequency bins cannot be detected. In this research, 1024-point FFT and 2.56 GHz ADC are applied, and the 20 bins in frequency domain represent 50 MHz, which means, the second signal has to be 50 MHz away from the first signal. Fig 4.3.3 and Fig 4.3.4 show the second signal is 7.5 MHz away from the first signal.

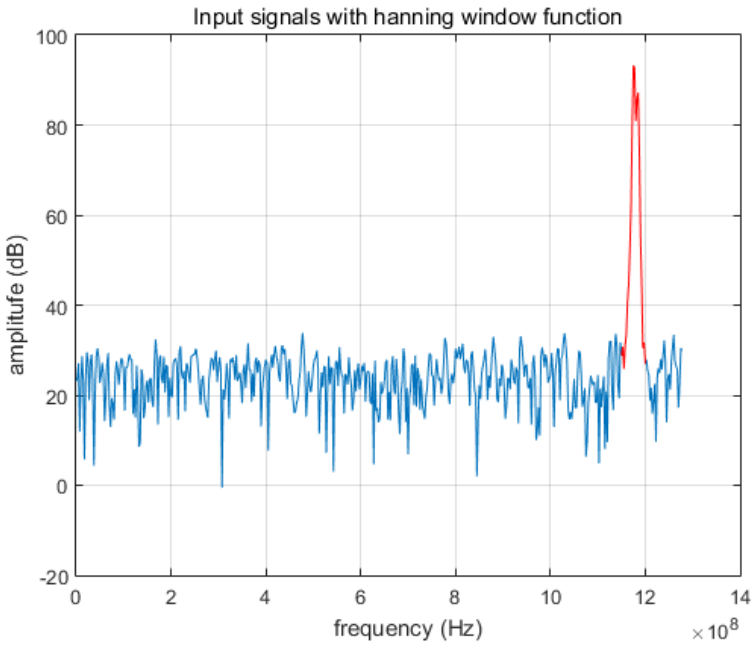

Fig 4.3.3 Two Inputs with 7.8 MHz Frequency Difference without Compensation

(f_1=1183.9 MHz and f_2=1176.1 MHz)

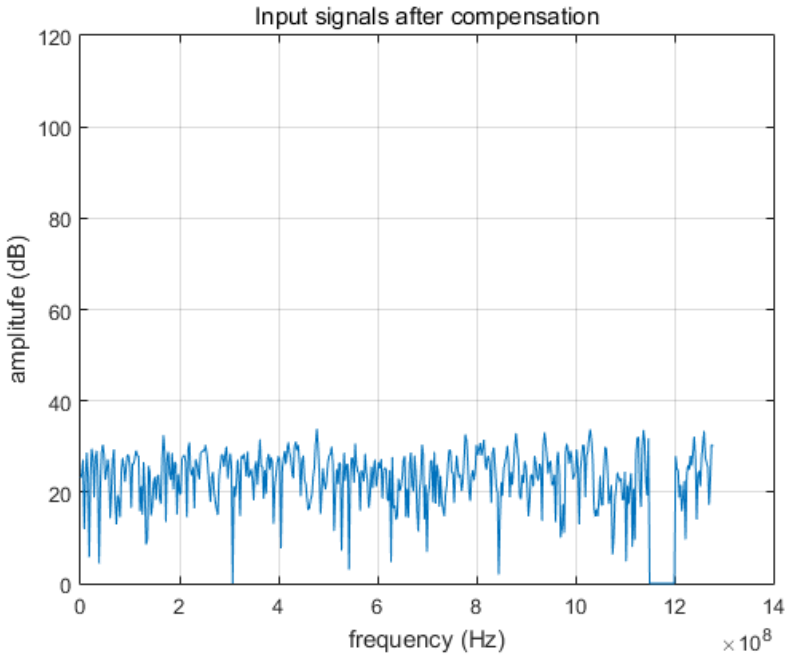

Fig 4.3.4 Two Inputs with 7.8 MHz Frequency Difference with Compensation

(f_1=1183.9 MHz and f_2=1176.1 MHz)

The actual frequencies of these two signals are 1183.9 MHz and 1176.1 MHz, and only the strong signal is detected. Thus, the compensation method cannot expose the second signal when two signals are close to each other.

The FFT spectrum for squared signal provides more information about the second signal. Fig 4.3.5 shows the squared data in frequency domain. Because of the two facts, the frequency difference between the two signals, 7.5 MHz, is detected in Fig 4.3.5 and the first signal detected in Fig 4.3.3. Therefore, the second signal exists and the frequency subtraction from the first signal is 7.5 MHz.

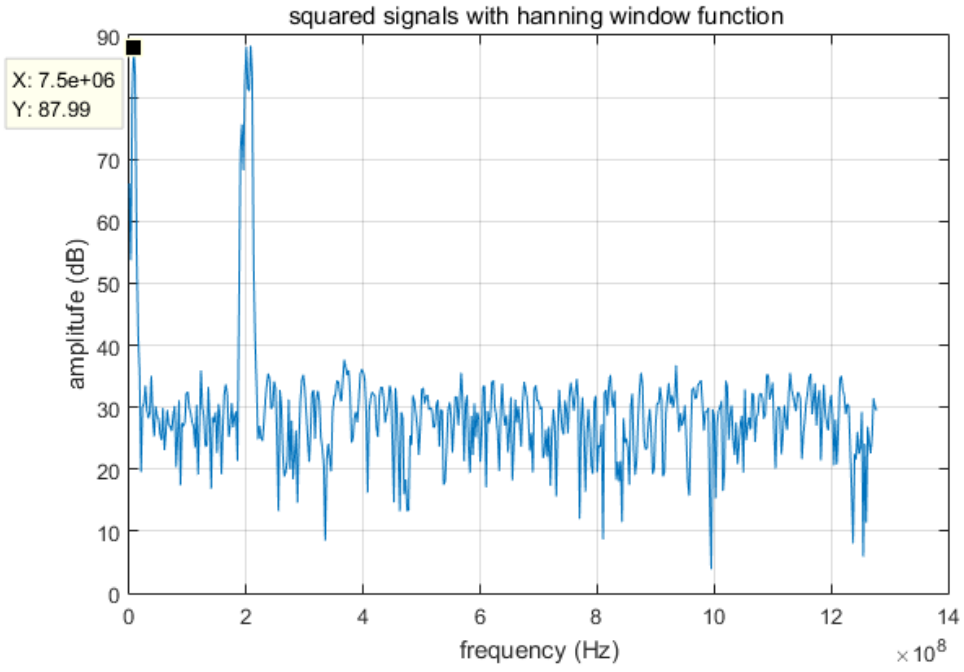

Fig 4.3.5 Squared Signals with Two Close Frequencies in Frequency Domain

4.3.2 The Second Signal Detection

After the second signal is verified, next is to find its frequency. As shown in Fig 4.3.6, two local peak signals are located at 1175 MHz and 1185 MHz, about 6

frequency bins away, which is very close to the two signal subtraction 7.5 MHz, 5 bins in Fig 4.3.5. Therefore, the second signal is detected and its frequency is 1175 MHz.

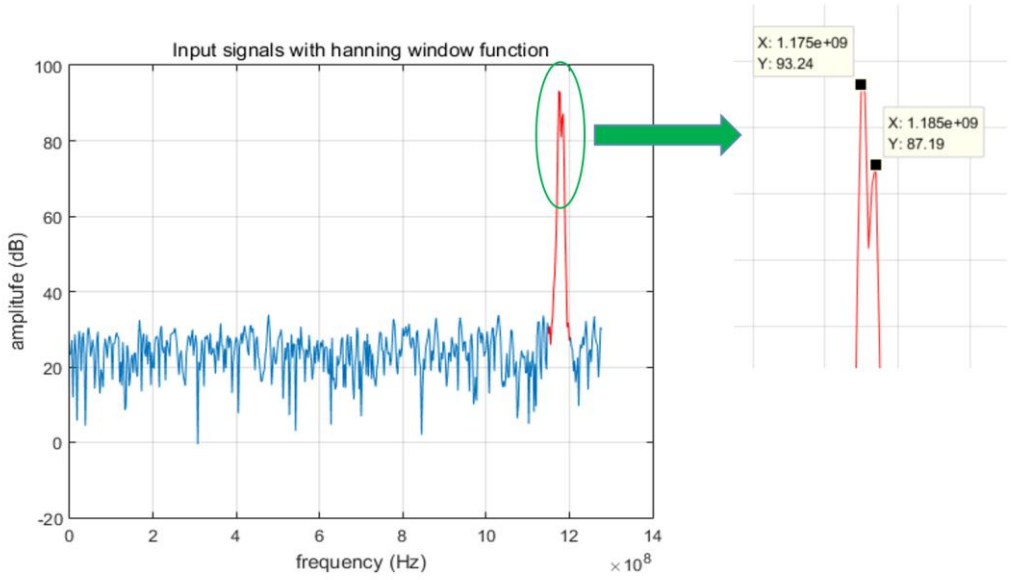

Fig 4.3. 6 Zooming in FFT Spectrum

The frequency of the second signal (close to the first signal f_1) may not be determined by the non-squared data when there is no local peak near f_1 in non-squared FFT spectrum (see example in Fig 4.3.7 and Fig 4.3.8). Excluding the frequency bin for the frequency subtraction, another peak could be detected in the squared FFT spectrum. In this research, the first local peak P_1 is a detectable local peak in the first 10 bins of the squared FFT spectrum which represents two signals' frequency subtraction. The second local peak P_2 is the next peak in the rest of the frequency bins and the third local peak P_3 is the maximum local peak near P_2. In this case, if the frequency of the strong signal is f_1 and the second signal is f_2, then P_2 is the location

of $2f_1$ or f_1+f_2. Since the f_1 is already detected by FFT spectrum, then P_2 must be f_1+f_2 if it is not located at $2f_1$. In our experiments, when the P_2 is more than 2 frequency bins away from $2f_1$, then f_2 is f_{P2} -f_1.

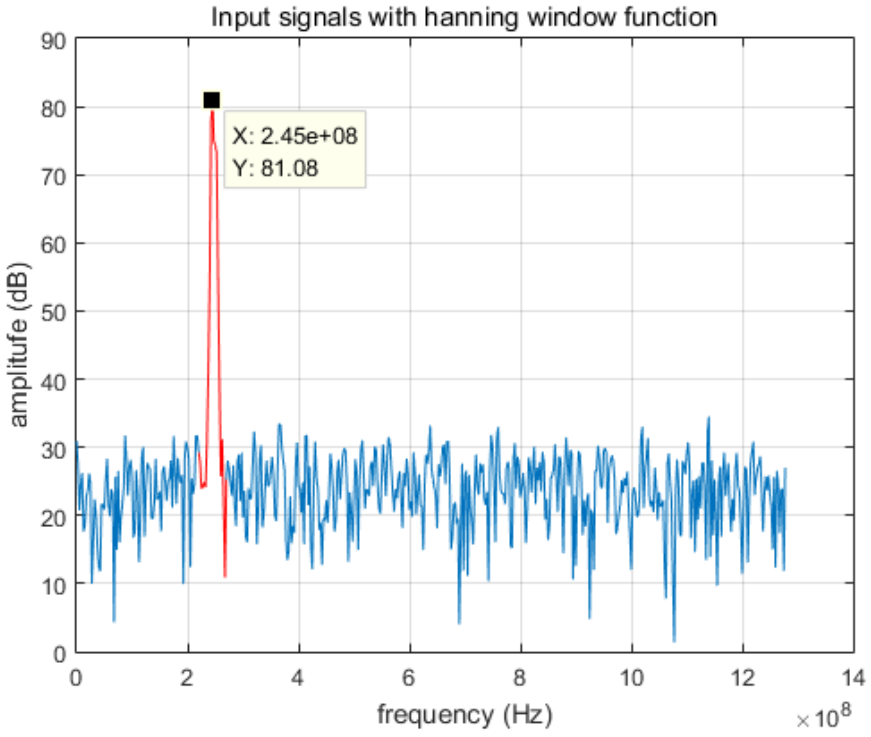

Fig 4.3.7 244.49 MHz and 250.88 MHz Non-squared FFT Spectrum

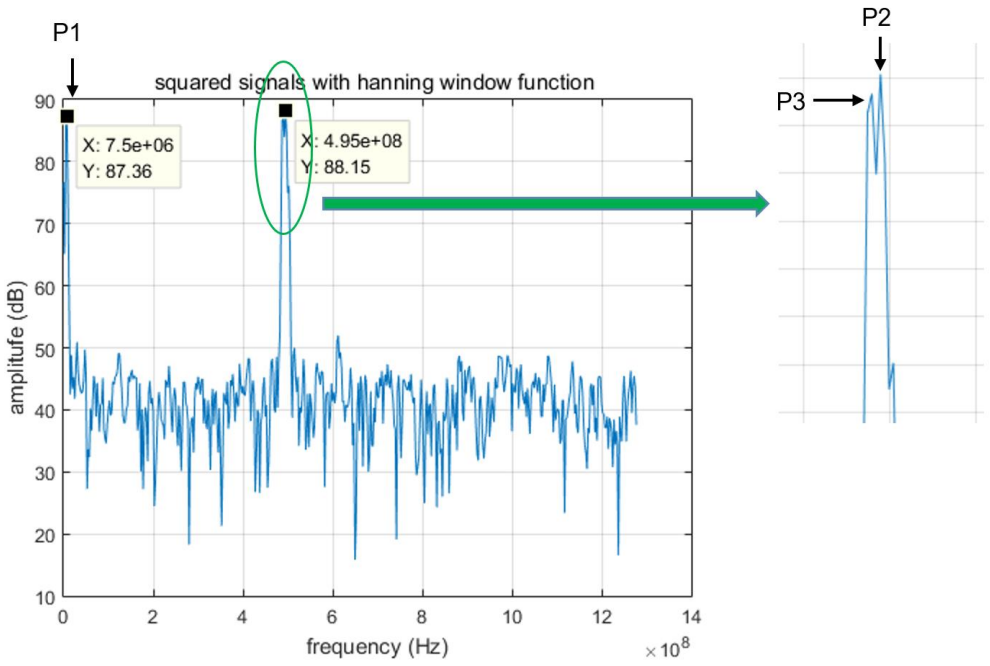

Fig 4.3.8 244.49 MHz and 250.88 MHz Squared FFT Spectrum

Another example of two input signals, 168.86 MHz and 161.92 MHz, is shown in Fig 4.3.9, where the second signal is not detected by the non-squared data. In this case, the squared signal in frequency domain is shown in Fig 4.3.10. It is evaluated to determine the second signal frequency by using the squared signal frequencies, i.e., f_1-f_2, f_1+f_2, $2f_1$ and $2f_2$, as shown in the following equations.

$$f_1 + f_2 = 2f_1 - (f_1 - f_2) \tag{4.3.1}$$

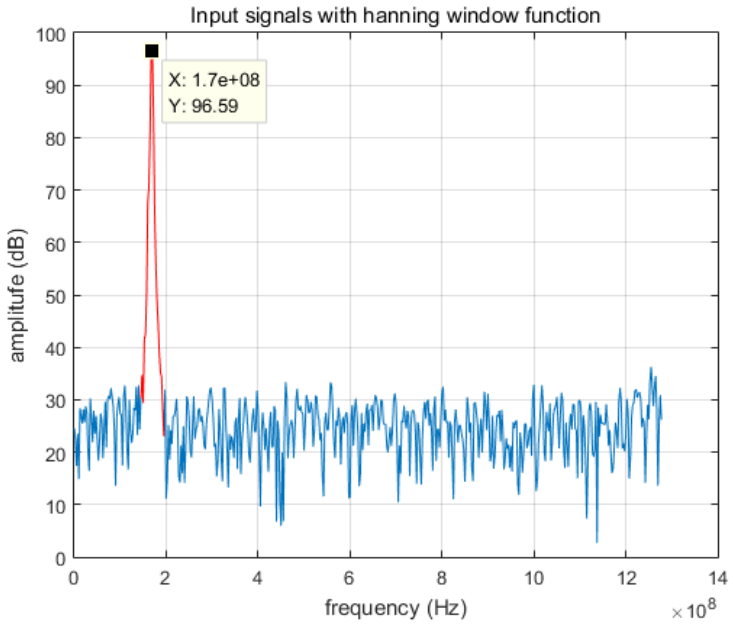

Fig 4.3.9 168.86 MHz and 161.92 MHz Non-squared FFT Spectrum

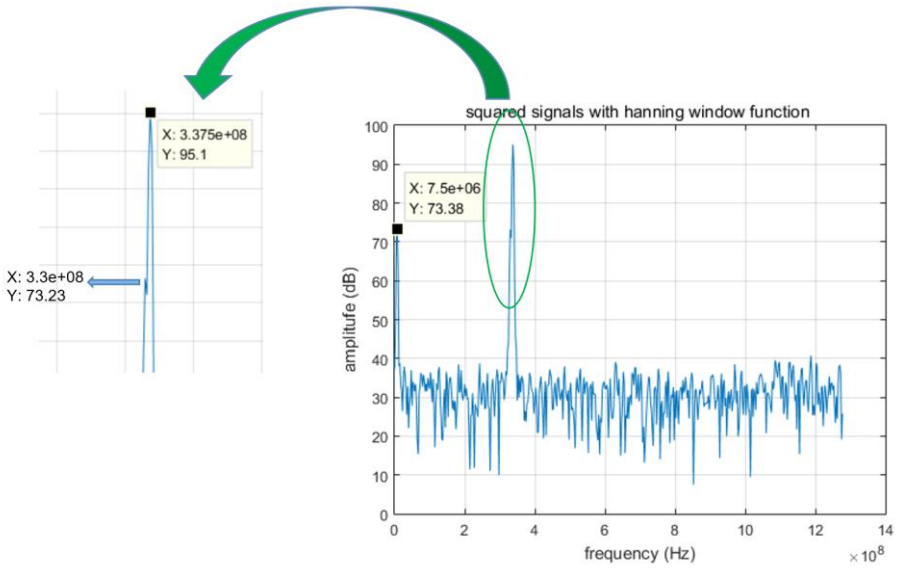

Fig 4.3.10 168.86 MHz and 161.92 MHz Squared FFT Spectrum

In Fig 4.3.10, the first local peak is 7.5 MHz, which verifies existence of the second signal and the frequency subtraction is 7.5 MHz. The next local peak is 337.5

MHz, which is 1 bin away from 340 MHz, double frequency of the strong signal. The third peak is 330 MHz, which is the frequency summation of the two signals. It is exactly 7.5 MHz away from 337.5 MHz. Evaluating all these data, the second signal frequency is determined to be 162.5 MHz by subtracting 7.5 MHz from the first signal frequency.

If the strong signal is greater than 640 MHz, then its double frequency is greater than half of the frequency span of FFT, 1.28 GHZ. Fig 4.3.11 and Fig 4.3.12 give an example of this case.

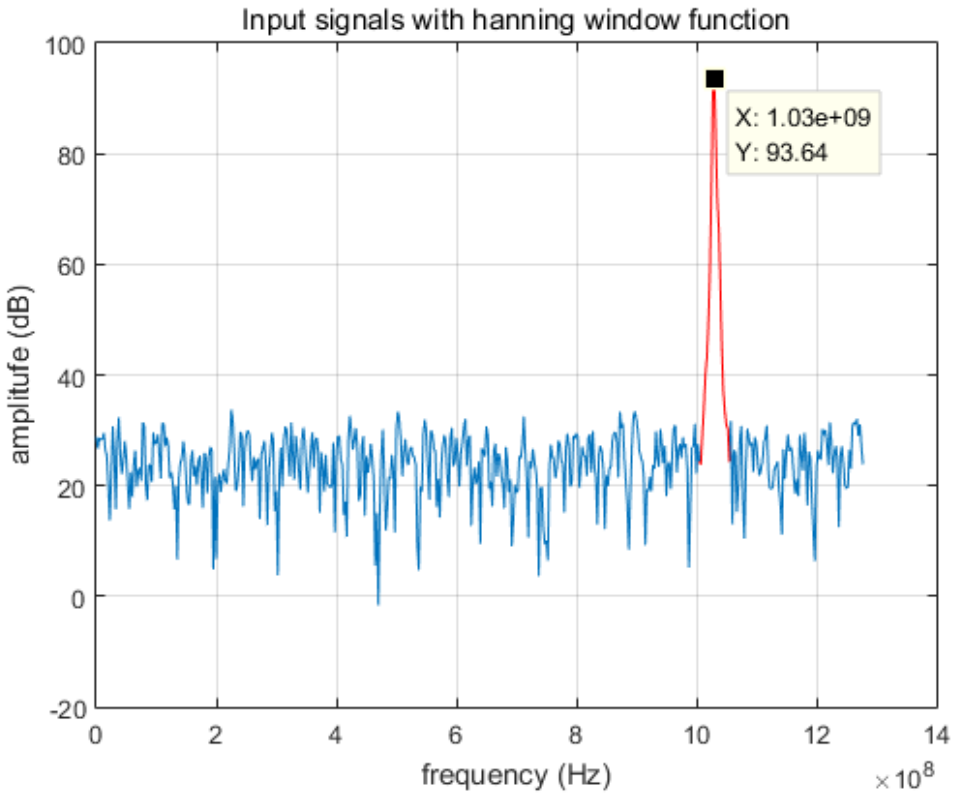

Fig 4.3.11 1029.2 MHz and 1036.2 MHz Non-squared FFT Spectrum

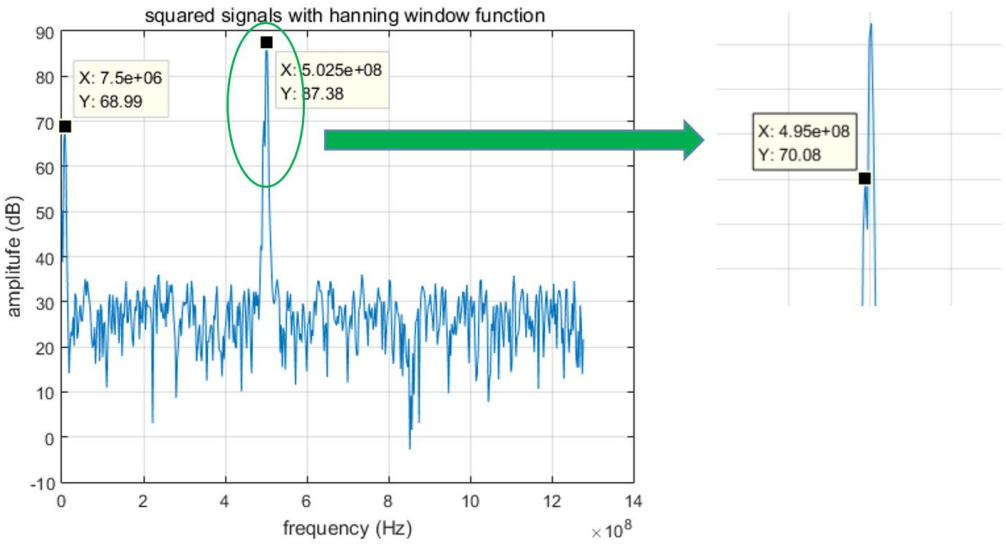

Fig 4.3.12 1029.2 MHz and 1036.2 MHz Squared FFT Spectrum

In Fig 4.3.12, the 502.5 MHz also can represent 2058 MHz, the double frequency of the first signal 1029.2 MHz, by considering full frequency span of FFT. A local 495 MHz is found, representing 2065 MHz as the frequency summation. So the second signal frequency is calculated as adding the frequency subtraction 7.5 MHz to the first signal frequency 1030 MHz, 1037.5 MHz.

In special cases, the frequency summation 1 bin away from the double frequency of the first signal, is not detected because of signal interference and spur. Then, the double frequency of the second signal needs to be evaluated to help determine the second signal frequency, by Eq. 4.3.2, Fig 4.3.13 and Fig 4.3.14

$$2f_2 = 2f_1 - 2(f_1 - f_2) \tag{4.3.2}$$

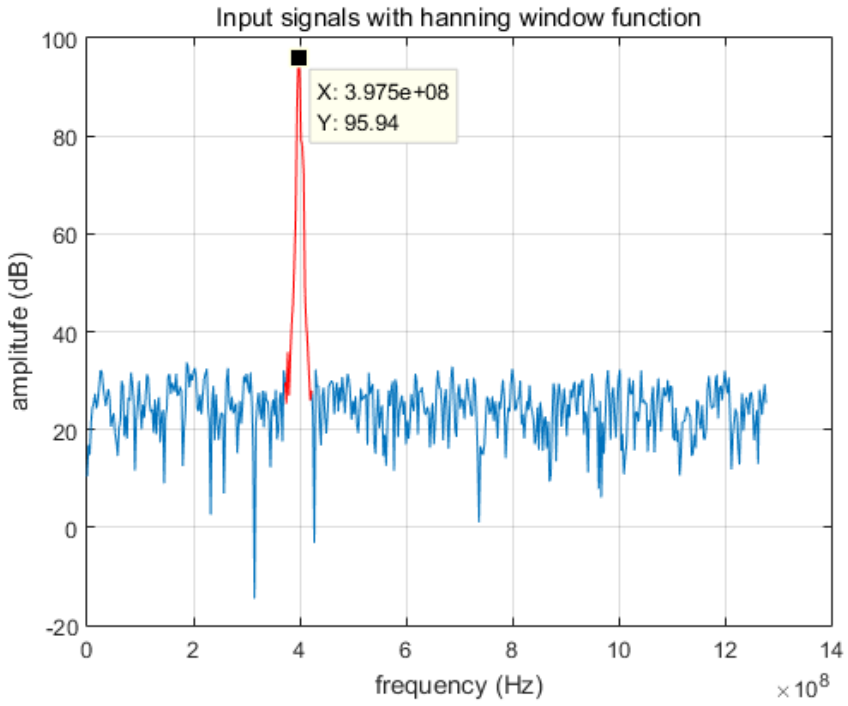

Fig 4.3.13 398.12 MHz and 404.76 MHz Non-squared FFT Spectrum

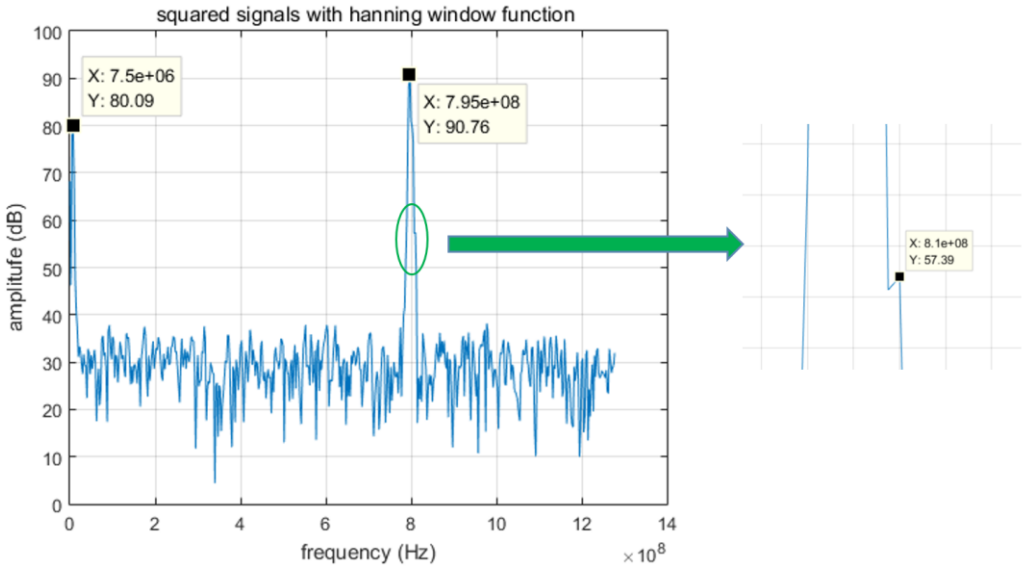

Fig 4.3.14 398.12 MHz and 404.76 MHz Squared FFT Spectrum

Noticing the 810 MHz is 7.5*2 MHz away from the 795 MHz, thus, the 810 MHz is double frequency of the second signal, which is 405 MHz.

If the two signals are very close to each other, 1 to 2 frequency bins away, then, the above analysis approach faces challenge. When the frequency subtraction is less than 5 MHz, a method to detect the second signal is introduced. Fig 4.3.15 and Fig 4.3.16 give an example when the two input signals are 2 bins away. The first signal frequency f_1 is 225 MHz and the frequency subtraction is 5 MHz. The peak 447.5 MHz is not exactly equal to $2f_1$, 450 MHz. Thus, the 447.5 MHz is considered as the frequency summation f_1+f_2, then the f_2 is 447.5 MHz – 225 MHz=222.5 MHz and the actual second signal frequency is 220.06 MHz.

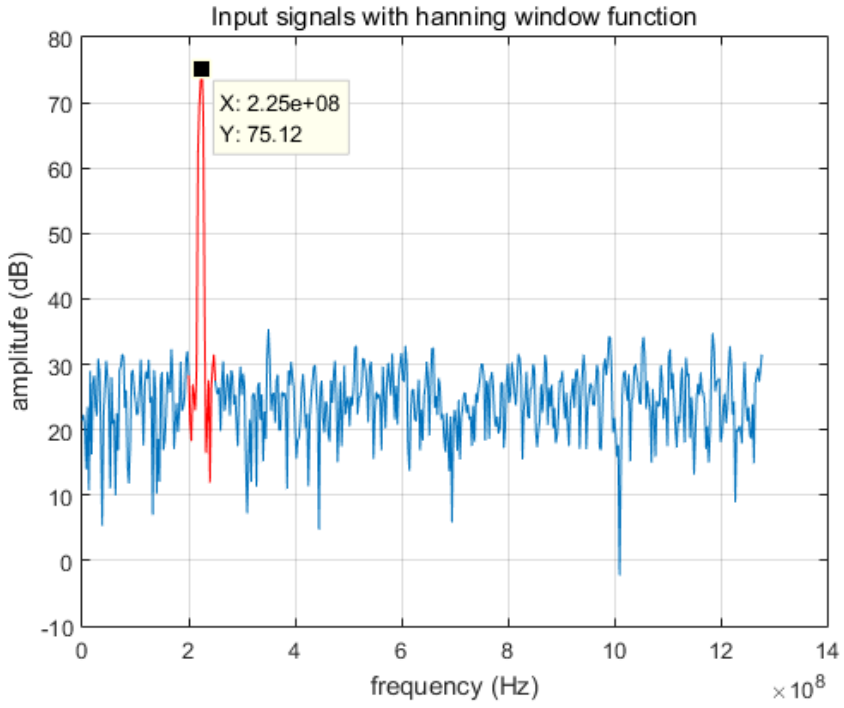

Fig 4.3.15 220.06 MHz and 224.78 MHz Non-squared FFT Spectrum

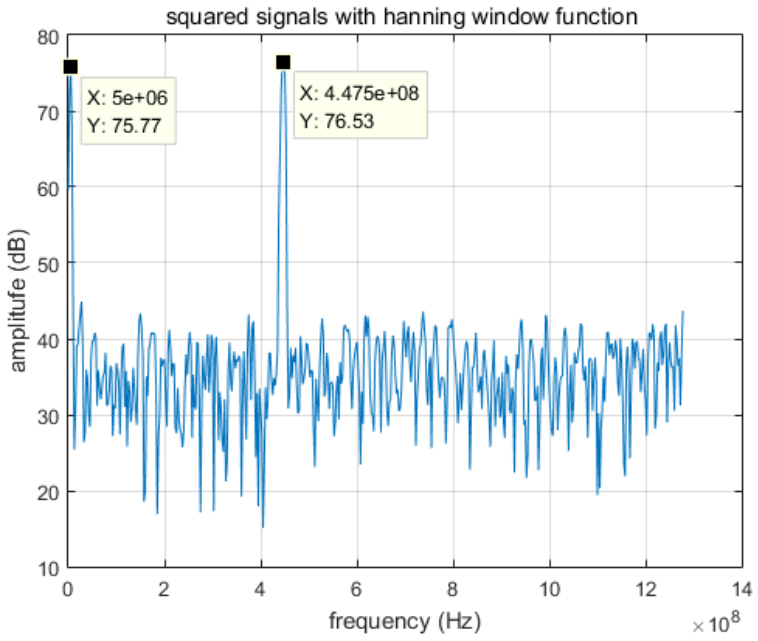

Fig 4.3.16 220.06 MHz and 224.78 MHz Squared FFT Spectrum

Another case of the second signal detection is shown in Fig 4.3.17 and Fig 4.3.18.

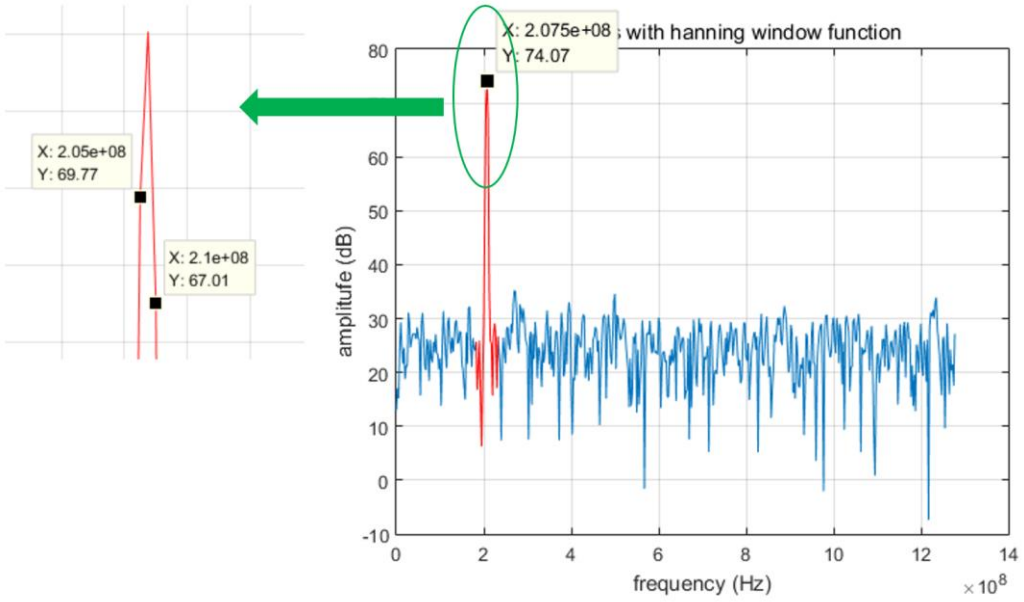

Fig 4.3.17 204.29 MHz and 207.36 MHz Non-squared FFT Spectrum

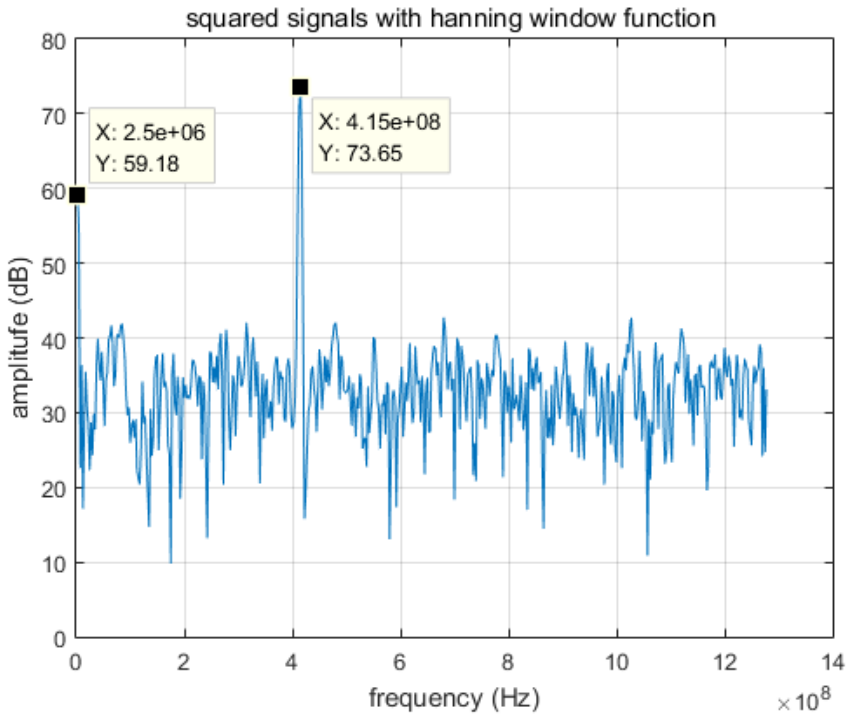

Fig 4.3.18 204.29 MHz and 207.36 MHz Squared FFT Spectrum

In this example, the detected peak 415 MHz is exactly the double frequency of f_1, 207.5 MHz, and the frequency subtraction is 2.5 MHz. The second signal frequency is calculated as 206.36 MHz using the fine frequency estimation. Since the left frequency bin of f_1 has a higher amplitude than the left frequency bin of f_1. The second signal frequency is set to f_1-f_{sub} which is 206.36-2.5=203.86 MHz.

As shown in Fig 4.3.19, the right frequency bin of f_1 has a higher amplitude than the left frequency bin of f_1, then the second signal frequency is set to f_1+f_{sub}.

4.4 Two Signals Detection Algorithm

As discussed in Section 4.3, the conditions for two signals detection is complicate, and multiple cases are considered. In this Section, several special

definitions are used in Fig 4.4.1. A two signals detection flow chart is depicted in Fig 4.4.2. The second signal frequency estimation flow chart is depicted in Fig 4.4.3.

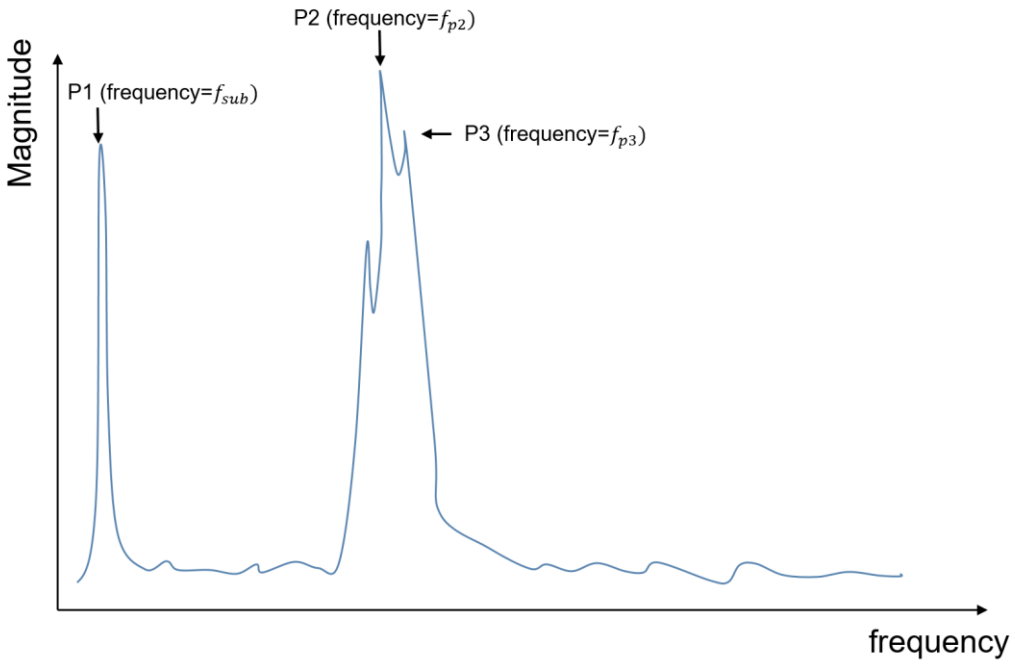

Fig 4.4.1 Spectrum for Special Definitions

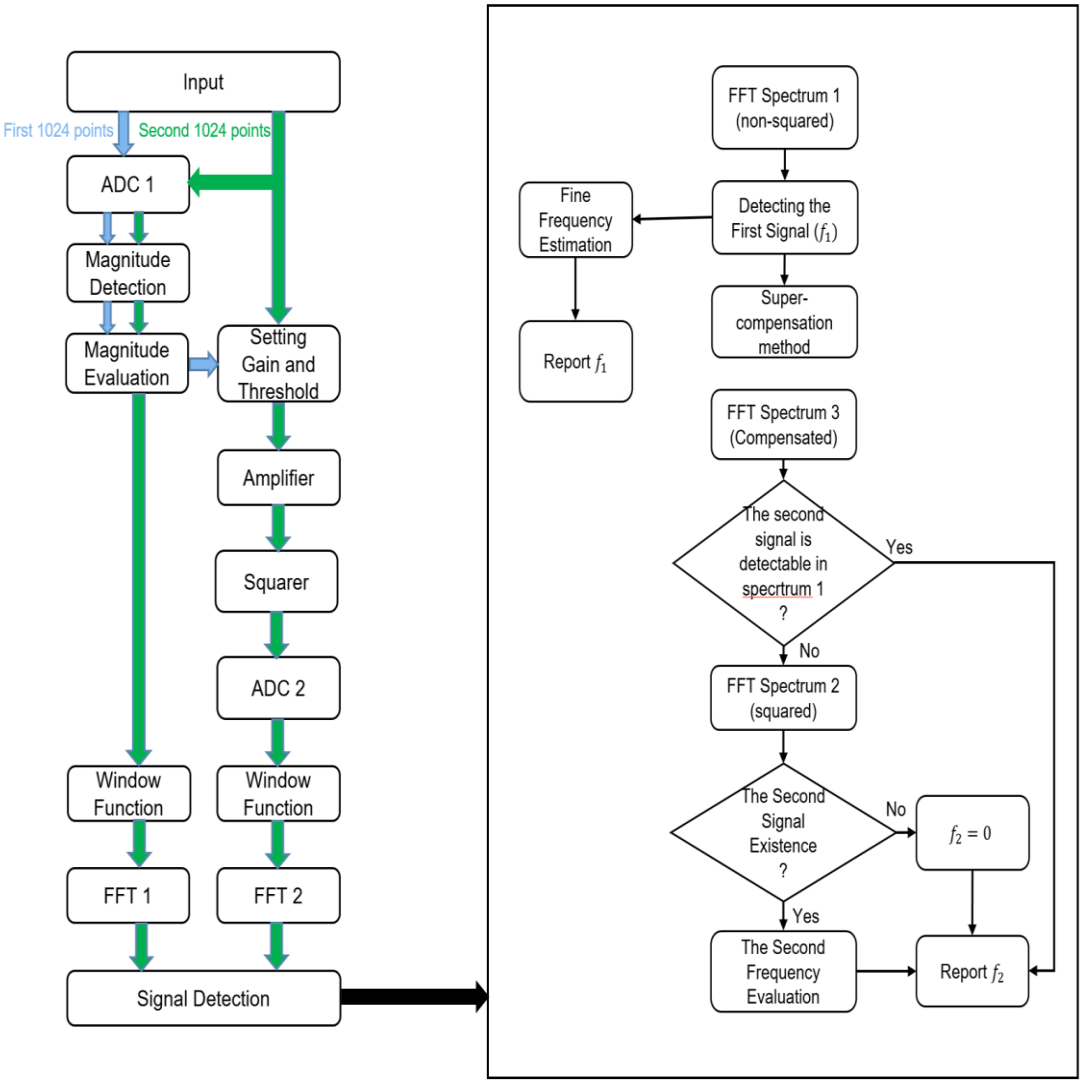

Fig 4.4.2 Two Signals Detection Flow Chart

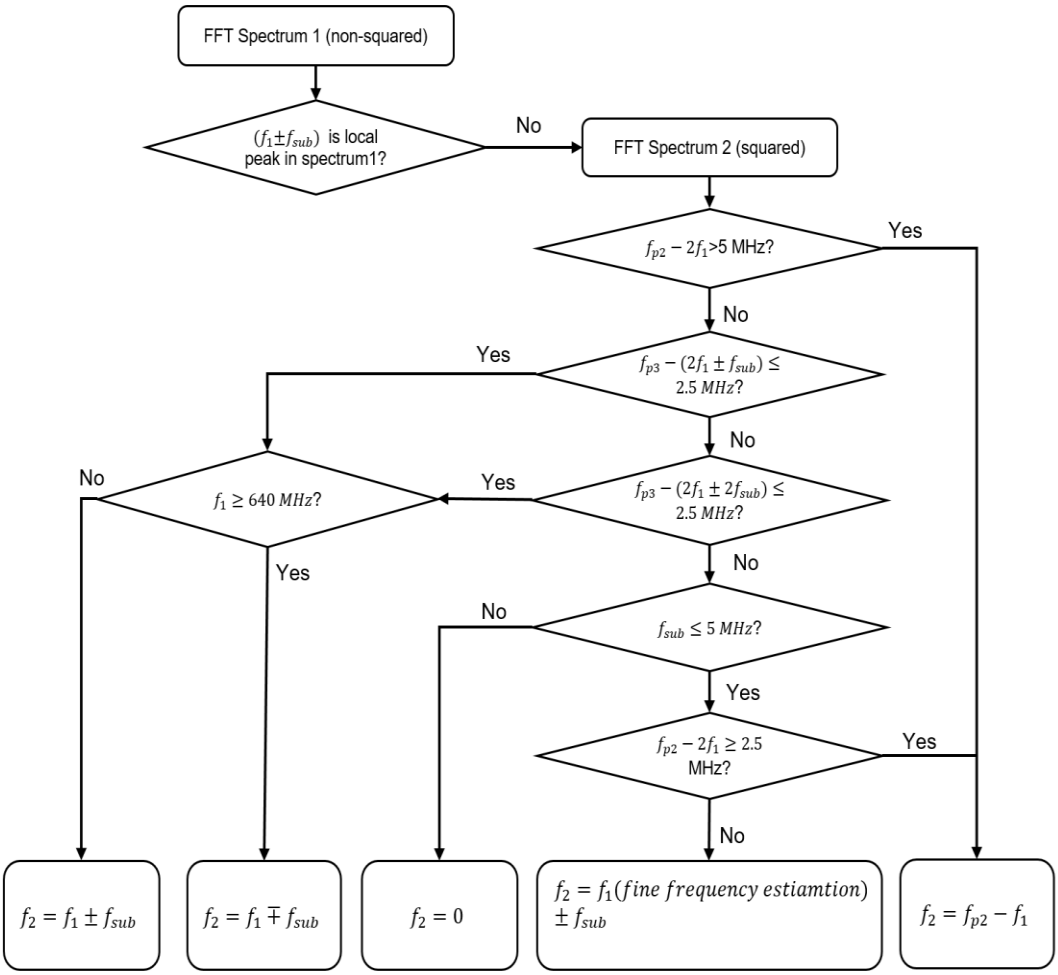

Fig 4.4.3 The Second Signal Frequency Evaluation

4.5 Experimental Results

Performance of two signals detection in the proposed receiver is evaluated by random signal frequency, phase and amplitudes with the weak signal SNR above -6.5. The frequency span of two signals is from 30 MHz to 1250 MHz. Table 4.1 summarizes the second signal detection results of receiver with and without Squarer. 10,000 simulation runs were conducted for every case listed in the table. Considering the second signal detection, the proposed receiver using Squarer improve 2% (200 of

10,000) cases with frequency accuracy < 2.5 MHz and about 0.2% (20 of 10,000) case with frequency accuracy < 5 MHz.

Table 4.1 Performance of the Second Signal Detection

Amplitude Summation (mV)	The Second Signal Detection Probability				
	Receiver w/o Squarer		Receiver with Squarer		
	Error<=2.5MHz	False Alarm	Error<=2.5MHz	2.5MHz<Error<=5MHz	False Alarm
2.9-17.4	0.9707	0	0.9948	0.0018	0
13.8-69.3	0.9763	0	0.9977	0.0011	0
61.7-195.4	0.972	0	0.997	0.0014	0
174-309.5	0.973	0	0.9969	0.0018	0
347.2-490.6	0.9754	0	0.997	0.0021	0

Table 4.2 summarizes the second signal detection results of receiver with and without Squarer where the input signal frequencies are close to each other.

Table 4.2 Fixed Range Amplitudes and Closed Frequencies

Amplitude Summation (mV)	The Second Signal Detection Probability						
	Frequency Subtraction 1.25MHz-6.25MHz			Frequency Subtraction 6.25MHz-16.25MHz			False Alarm
	Receiver w/o Squarer	Receiver with Squarer		Ordinary Receiver	Receiver with Squarer		
	Error<=2.5MHz	Error<=2.5MHz	2.5MHz<Error<=5MHz	Error<=2.5MHz	Error<=2.5MHz	2.5MHz<Error<=5MHz	
2.9-17.4	0	0.743	0.1885	0.0318	0.9094	5.60E-04	0
13.8-69.3	0	0.7276	0.1953	0.0304	0.9529	1.50E-04	0
61.7-195.4	0	0.7343	0.1932	0.0299	0.9631	8.00E-05	0
174-309.5	0	0.7641	0.1725	0.0297	0.979	2.00E-05	0
347.2-490.6	0	0.7588	0.1791	0.0308	0.9939	1.00E-04	0

V. Conclusion

Modern wideband receiver systems are demanded to detect multiple signals in a high dynamic range and frequency resolution environment. Conventional Fast Fourier Transform (FFT) based receivers have capability of detection multiple signals; however, a limitation is these detectable signals would have to be separated at least five frequency bins away from each other in FFT frequency spectrum. If two simultaneous signals are close within five frequency bins then the second signal is hidden in the main lobe of the strong one and cannot be detected. In this thesis, a high frequency resolution adaptive thresholding wideband receiver system is presented, which accurately detects two simultaneous high dynamic range signals close to one frequency bin. The receiver design architecture and performance evaluation are presented.

Hardware implementation of this receiver system using FPGA and GPU will be studied in the future.

References

[1] C.-I. H. Chen, K. George, W. McCormick and J. B. Y. Tsui, "Design and Performance Evaluation of a 2.5-GSPS Digital Receiver," *IEEE Transactions on Instrumentation and Measurement,* vol. 54, no. 3, pp. 1089-1099, June 2005.

[2] K. George and C.-i. H. Chen, "Multiple Signal Detection Digital Wideband Receiver using Hardware Accelerators," *IEEE Transactions on Aerospace and Electronic Systems,* vol. 49, no. 2, pp. 706-715, April 2013.

[3] G. D. Bergland, "A Radix-Eight Fast-Fourier Transform Subroutine for Real-Valued Series," *IEEE Transactions on Audio and Electroacoustics,* vol. 17, no. 2, pp. 138-144, June 1969.

[4] P. Duhamer and H. Hollmann, "Split Radix FFT Algorithm," *Electronics Leteers,* January 1984.

[5] R. C. Singleton, "An Algorithm for Computing the Mixed Radix Fast Fourier Transform," *IEEE Transaction on Audio Electroacoust,* June 1969.

[6] D. S. K. Pok, C.-I. H. Chen, J. J. Schamus, C. T. Montgomery and J. B. Y. Tsui, "Chip Design for Monobit Receiver," *IEEE Transactions on Microwave Theory and Techniques,* vol. 45, no. 12, pp. 2283-2295, December 1997.

[7] Y.-H. Lee and C.-I. Chen, "Dual thresholding for digital wideband receivers with variable truncation scheme," in *IEEE International Symposium on Circuits and Systems*, 2009.

[8] K. George, C.-I. H. Chen and J. B. Y. Tsui, "Extension of Two-Signal Spurious-Free Dynamic Range of Wideband Digital Receivers Using Kaiser Window and Compensation Method," *IEEE Transactions on Microwave Theory and Techniques,* vol. 55, no. 4, pp. 788-794, April 2007.

[9] K. George and C.-I. H. Chen, "Multiple Signal Detection and Measurement Using a Configurable Wideband Digital Receiver," in *Instrumentation and Measurement Technology Conference*, 2007.

[10] R. Hidayat, K. Dejhan, P. Moungnoul and Y. Miyanaga, "A GHz Simple CMOS Squarer Circuit," in *International Symposium on Communications and Information Technologies* , 2008.

[11] K.-J. Cho, Y.-E. Kim and J.-G. Chung, "Power and Area Efficient Squarer Design," in *Fortieth Asilomar Conference on Signals, Systems and Computers*, 2006.

[12] M. Parvizi, K. Allidina and M. N. El-Gamal, "An Ultra Low Power, Low Voltage CMOS Squarer," in *IEEE International Symposium on Circuits and Systems*, 2012.

[13] D. M. Lin and L. L. Liou, "Two signal high dynamic range and high resolution wideband digital receiver using beat frequency," in *IEEE Military Communications Conference*, 2008.

[14] S. Benson and C.-I. H. Chen, "Adaptive thresholding for high dual-tone signal instantaneous dynamic range in digital wideband receive," in *IEEE Instrumentation and Measurement Technology Conference*, 2010.

[15] J. Tsui, Special Design Topics in Digital Wideband Receivers, 2010.

[16] Y.-H. G. Lee and C.-I. H. Chen, "Dual thresholding for digital wideband receivers with variable truncation scheme," in *IEEE International Symposium on Circuits and Systems*, 2009.